Contents

Chapter 14

Vorticity

Box 14.1
Reader's Guide

- This chapter relies heavily on Chap. 12, *Fundamentals of Fluid Dynamics.*

- Chapters 14–18 (fluid mechanics and magnetohydrodynamics) are extensions of this chapter; to understand them, this chapter must be mastered.

- Portions of Part V, Plasma Physics (especially Chap. 20 on the "two-fluid formalism"), rely on this chapter.

14.1 Overview

In the last chapter, we introduced an important quantity called *vorticity* which is the subject of the present chapter. Although the most mathematically simple flows are "potential flows", with velocity of the form $\mathbf{v} = \boldsymbol{\nabla}\psi$ for some ψ so the vorticity $\boldsymbol{\omega} = \boldsymbol{\nabla} \times \mathbf{v}$ vanishes, the majority of naturally occuring flows are vortical. We shall find that studying vorticity allows us to develop an intuitive understanding of how flows evolve. Furthermore, computing the vorticity can provide an important step along the path to determining the full velocity field of a flow.

We all think we know how to recognise a vortex. The most hackneyed example is water disappearing down a drainhole in a bathtub or shower. Here what happens is that the angular velocity around the drain increases inward, because the angular momentum per unit mass is conserved when the water slowly circulates radially in addition to rotating. This angular momentum conservation means that the product of the circular velocity v_ϕ and the

radius ϖ is independent of radius, which, in turn, implies that $\boldsymbol{\nabla} \times \mathbf{v} \simeq 0$. So this is a vortex without much vorticity! (except, as we shall see, a delta-function spike of vorticity right at the drainhole's center); see Fig. 14.1 and Ex. 14.14. Vorticity is a precise physical quantity defined by $\boldsymbol{\omega} = \boldsymbol{\nabla} \times \mathbf{v}$, not any vaguely circulatory motion.

In Sec. 14.2, we introduce two tools for analyzing and utilizing vorticity: vortex lines, and circulation. Vorticity is a vector field, and therefore has integral curves obtained by solving $d\mathbf{x}/d\lambda = \boldsymbol{\omega}$ for some parameter λ. These integral curves are the *vortex lines*; they are analogous to magnetic field lines. The flux of vorticity $\int \boldsymbol{\omega} \cdot d\boldsymbol{\Sigma}$ across a closed surface is equal to the integral of the velocity field $\int \mathbf{v} \cdot d\mathbf{x}$ around the surface's boundary (by Stokes' theorem). We call this the *circulation*; it is analogous to magnetic-field flux. In fact, the analogy with magnetic fields turns out to be extremely useful. Vorticity, like a magnetic field, automatically has vanishing divergence, which means that the vortex lines are continuous, just like magnetic field lines. Vorticity, again like a magnetic field, is an axial vector and thus can be written as the curl of a polar vector potential, the velocity $\mathbf{v}$.[1] Vorticity has the interesting property that it evolves in a perfect fluid in such a manner that the flow carries the vortex lines along with it; we say that the vortex lines are "frozen into the fluid". When viscous stresses make the fluid imperfect, then the vortex lines diffuse through the moving fluid with a diffusion coefficient that is equal to the kinematic viscosity ν.

In Sec. 14.3, we study a classical problem that illustrates both the action and the propagation of vorticity: the *creeping* flow of a low Reynolds number fluid around a sphere. (Low-Reynolds-number flow arises when the magnitude of the viscous stress in the equation of motion is much larger than the magnitude of the inertial acceleration.) The solution to this problem finds contemporary application in computing the sedimentation rates of soot particles in the atmosphere.

In Sec. 14.4, we turn to high Reynolds number flows, in which the viscous stress is quantitatively weak over most of the fluid. Here, the action of vorticity can be concentrated in relatively thin *boundary layers* in which the vorticity, created at the wall, diffuses away into the main body of the flow. Boundary layers arise because in real fluids, intermolecular attraction requires that the component of the fluid velocity parallel to the boundary (not just the normal component) vanish. It is the vanishing of both components of velocity that distinguishes real fluid flow at high Reynolds number (i.e. small viscosity) from the solutions obtained assuming vanishing vorticity. Nevertheless, it is often a good approximation to adopt a solution to the equations of fluid dynamics in which vortex-free fluid slips freely past the solid and then match it onto the solid using a boundary-layer solution.

Stirred water in a teacup and the Earth's oceans and atmosphere rotate nearly rigidly, and so are most nicely analyzed in a co-rotating reference frame. In Sec. 14.5 we use such an analysis to discover novel phenomena produced by Coriolis forces — including winds around pressure depressions, "Taylor columns" of fluid that hang together in a rigid-body-like way, "Ekman boundary layers" with spiral-shaped velocity fields, gyres such as the Sargasso Sea around which ocean currents such as the Gulf Stream circulate, and tea leaves that

---

[1]Pursuing the electromagnetic analogy further we can ask the question, "Given a specified vorticity field $\boldsymbol{\omega}(\mathbf{x}, t)$ can I solve uniquely for the velocity $\mathbf{v}(\mathbf{x}, t)$?" The answer, of course is "No". There is gauge freedom and many solutions exist. Interestingly, if we specify that the flow be incompressible $\boldsymbol{\nabla} \cdot \mathbf{v} = 0$ (i.e. be in the analog of Coulomb gauge), then $\mathbf{v}(\mathbf{x}, t)$ is unique.

accumulate at the bottom center of a tea cup.

When a flow has a large amount of shear, Nature often finds ways to tap the relative kinetic energy of neighboring stream tubes. In Sec. 14.6 we explore the resulting instabilities, focusing primarily on horizontally stratified fluids with relative horizontal velocities, which have vorticity concentrated in regions where the velocity changes sharply. The instabilities we encounter show up, in Nature, as (among other things) "billow clouds", clear-air turbulence in the stratosphere, and the driving of ocean waves by wind. These phenomena will provide motivation for the principal topic of the next chapter: turbulence.

Physical insight into the phenomena of this chapter is greatly aided by movies of fluid flows. The reader is urged to view relevant movies in parallel with reading this chapter; see Box 14.2

Box 14.2
Movies Relevant to this Chapter

In the 1960s, the National Committee for Fluid Mechanics Films produced a set of movies that are pedagogically powerful and still fully relevant, a half century later. These movies are currently (2012) available on the web at `http://web.mit.edu/hml/ncfmf.html`. Those most relevant to this chapter are:

- *Vorticity*, by Ascher Shapiro (1961) – relevant to the entire chapter.

- *Low Reynolds Number Flows*, by Sir Geoffrey Taylor (1964a) – relevant to Sec. 14.3 of this chapter.

- *Fundamental of Boundary Layers* by Frederick H. Abernathy (1968) – the portion dealing with (nonturbulent) laminar boundary layers, relevant to Sec. 14.4 of this chapter.

- *Rotating Flows*, by Dave Fultz (1969) – relevant to Sec. 14.5.

- *Secondary Flows*, by Edward S. Taylor (1964b) – relevant to circulation produced by Ekman boundary layers: Sec. 14.5.4.

14.2   Vorticity and Circulation

In Sec. 13.5.4 we defined the vorticity as the curl of the velocity field, $\boldsymbol{\omega} = \boldsymbol{\nabla} \times \mathbf{v}$, analogous to defining the magnetic field as the curl of a vector potential. To get insight into vorticity, consider the three simple 2-dimensional flows shown in Fig. 14.1:

Fig. 14.1(a) shows uniform rotation with angular velocity $\boldsymbol{\Omega} = \Omega \mathbf{e}_z$. The velocity field is $\mathbf{v} = \boldsymbol{\Omega} \times \mathbf{x}$, where $\mathbf{x}$ is measured from the rotation axis. Taking its curl, we discover that $\boldsymbol{\omega} = 2\boldsymbol{\Omega}$ everywhere.

Fig. 14.1(b) shows a flow in which the angular momentum per unit mass $\mathbf{j} = j\mathbf{e}_z$ is constant because it was approximately conserved as the fluid gradually drifted inward to
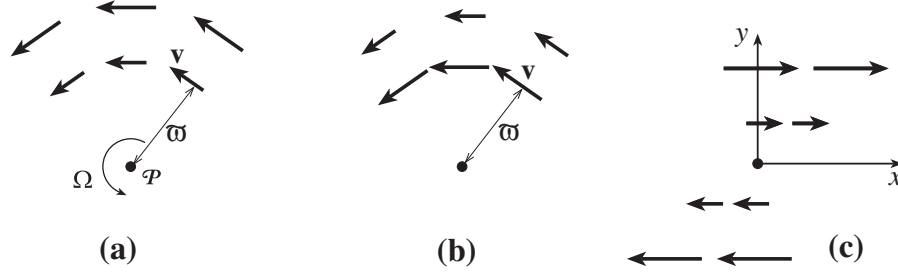
Fig. 14.1: Illustration of vorticity in three two-dimensional flows. The vorticity vector points in the z direction (orthogonal to the plane of the flow) and so can be thought of as a scalar ($\omega = \omega_z$). (a) Constant angular velocity Ω. If we measure radius ϖ from the center $\mathcal{P}$, the circular velocity satisfies $v = \Omega\varpi$. This flow has vorticity $\omega = 2\Omega$ everywhere. (b) Constant angular momentum per unit mass j, with $v = j/\varpi$. This flow has zero vorticity except at its center, $\omega = 2\pi j\delta(\mathbf{x})$. (c) Shear flow in a laminar boundary layer, $v_x = \omega y$. In this flow the vorticity is $\omega = v_x/y$.

create this flow. In this case, $\mathbf{v} = \mathbf{j} \times \mathbf{x}/\varpi^2$ (where $\varpi = |\mathbf{x}|$ and $\mathbf{j} =$constant). This is the kind of flow that occurs around a bathtub vortex, and around a tornado — but outside the vortex's and tornado's core. In this case, the vorticity is $\boldsymbol{\omega} = (\mathbf{j}/2\pi)\delta(\mathbf{x})$, i.e. it vanishes everywhere except at the center, $\mathbf{x} = 0$ (or, more precisely, except in the vortex's or tornado's core). What is different in this case is that the fluid rotates differentially and, although two neighboring fluid elements, separated tangentially, rotate about each other with an angular velocity $\mathbf{j}/\varpi^2$, when the two elements are separated radially, their angular velocity is $-\mathbf{j}/\varpi^2$. The average of these two angular velocities vanishes, so the vorticity vanishes.

The vanishing vorticity in this case is an illustration of a simple geometrical description of vorticity in any two dimensional flow (Ex. **??**): If we orient the $\mathbf{e}_z$ axis of a Cartesian coordinate system along the vorticity, then

$$\omega = \left(\frac{\partial v_y}{\partial x} - \frac{\partial v_x}{\partial y}\right)\mathbf{e}_z \ . \tag{14.1}$$

This expression implies that the vorticity at a point is the sum of the angular velocities of a pair of mutually perpendicular, infinitesimal lines passing through that point (one along the x direction, the other along the y direction) and moving with the fluid; for example, these lines could be thin straws suspended in the fluid. If we float a little vane with orthogonal fins in the flow, with the vane parallel to $\boldsymbol{\omega}$, then the vane will rotate with an angular velocity that is the average of the flow's angular velocities at its fins, which is half the vorticity. Equivalently, the vorticity is twice the rotation rate of the vane. In the case of constant angular momentum flow in Fig. 14.1(b), the average of the two angular velocities is zero, the vane doesn't rotate, and the vorticity vanishes.

Figure 14.1(c) shows the flow in a plane-parallel shear layer. In this case, a line in the flow along the x direction does not rotate, while a line along the y direction rotates with angular velocity ω. The sum of these two angular velocities, $0 + \omega = \omega$ is the vorticity. Evidently, curved streamlines are not a necessary condition for vorticity.

14.2.1 Vorticity Transport Equation

By analogy with magnetic field lines, we define a flow's *vortex lines* to be parallel to the vorticity vector $\boldsymbol{\omega}$ and to have a line density proportional to $\omega = |\boldsymbol{\omega}|$. These vortex lines will always be continuous throughout the fluid because the vorticity field, like the magnetic field, is a curl and therefore is necessarily solenoidal ($\boldsymbol{\nabla} \cdot \boldsymbol{\omega} = 0$). However, vortex lines can begin and end on solid surfaces, as the equations of fluid dynamics no longer apply there. Vorticity depends on the velocity field at a particular instant, and will evolve with time as the velocity field evolves. We can determine how by manipulating the Navier Stokes equation , which, for general, compressible flows, takes the form $\rho d\mathbf{v}/dt = -\boldsymbol{\nabla} P - \rho \boldsymbol{g} + \boldsymbol{\nabla}(\zeta \theta) + 2\boldsymbol{\nabla} \cdot (\eta \boldsymbol{\sigma})$ [Eq. (13.69)]. We shall keep matters simple throughout this chapter by assuming that the bulk viscosity is ignorable and the coefficient of shear viscosity is constant (which are usually fairly good assumptions). Then, even if the fluid is compressible, the Navier Stokes equation takes on the simplified form

$$\boxed{\frac{d\mathbf{v}}{dt} \equiv \frac{\partial \mathbf{v}}{\partial t} + (\mathbf{v} \cdot \boldsymbol{\nabla})\mathbf{v} = -\frac{\boldsymbol{\nabla} P}{\rho} - \boldsymbol{\nabla}\Phi + \nu\nabla^2 \mathbf{v}} \tag{14.2}$$

[Eq. (13.70)]. We take the curl of Eq. (14.2) and use the vector identity $(\mathbf{v}\cdot\boldsymbol{\nabla})\mathbf{v} = \boldsymbol{\nabla}(v^2)/2 - \mathbf{v} \times \boldsymbol{\omega}$ (easily derivable using the Levi-Civita tensor and index notation) to obtain

$$\frac{\partial \boldsymbol{\omega}}{\partial t} = \boldsymbol{\nabla} \times (\mathbf{v} \times \boldsymbol{\omega}) - \frac{\boldsymbol{\nabla} P \times \boldsymbol{\nabla} \rho}{\rho^2} + \nu\nabla^2 \boldsymbol{\omega}. \tag{14.3}$$

It is convenient to rewrite this vorticity evolution law with the aid of the relation (again derivable using the Levi-Civita tensor)

$$\boldsymbol{\nabla} \times (\mathbf{v} \times \boldsymbol{\omega}) = (\boldsymbol{\omega} \cdot \boldsymbol{\nabla})\mathbf{v} + \mathbf{v}(\boldsymbol{\nabla} \cdot \boldsymbol{\omega}) - \boldsymbol{\omega}(\boldsymbol{\nabla} \cdot \mathbf{v}) - (\mathbf{v} \cdot \boldsymbol{\nabla})\boldsymbol{\omega} . \tag{14.4}$$

Inserting this into Eq. (14.3), using $\boldsymbol{\nabla} \cdot \boldsymbol{\omega} = 0$ and introducing a new type of time derivative[2]

$$\boxed{\frac{D\boldsymbol{\omega}}{Dt} = \frac{\partial \boldsymbol{\omega}}{\partial t} + (\mathbf{v} \cdot \boldsymbol{\nabla})\boldsymbol{\omega} - (\boldsymbol{\omega} \cdot \boldsymbol{\nabla})\mathbf{v} = \frac{d\boldsymbol{\omega}}{dt} - (\boldsymbol{\omega} \cdot \boldsymbol{\nabla})\mathbf{v}} , \tag{14.5}$$

we bring Eq. (14.3) into the following form:

$$\boxed{\frac{D\boldsymbol{\omega}}{Dt} = -\boldsymbol{\omega}\boldsymbol{\nabla} \cdot \mathbf{v} - \frac{\boldsymbol{\nabla} P \times \boldsymbol{\nabla} \rho}{\rho^2} + \nu\nabla^2 \boldsymbol{\omega}} . \tag{14.6}$$

This is our favorite form for the vorticity evolution law for a compressible fluid with negligible bulk viscosity and constant shear viscosity. In the remainder of this section we shall explore its predictions.

The operator D/Dt (defined by Eq. (14.5) when acting on a vector and by $D/Dt = d/dt$ when acting on a scalar) is called the *fluid derivative*. (The reader should be warned that

---

[2]The combination of spatial derivatives appearing here is called the "Lie derivative" and denoted $\mathcal{L}_{\mathbf{v}}\boldsymbol{\omega} \equiv (\mathbf{v} \cdot \boldsymbol{\nabla})\boldsymbol{\omega} - (\boldsymbol{\omega} \cdot \boldsymbol{\nabla})\mathbf{v}$; it is also the "commutator" of $\mathbf{v}$ and $\boldsymbol{\omega}$ and denoted $[\mathbf{v}, \boldsymbol{\omega}]$. It is often encountered in differential geometry.
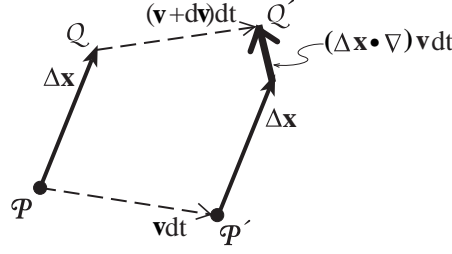
Fig. 14.2: Equation of motion for an infinitesimal vector $\Delta\mathbf{x}$ connecting two fluid elements. As the fluid elements at $\mathcal{P}$ and $\mathcal{Q}$ move to $\mathcal{P}'$ and $\mathcal{Q}'$ in a time interval dt, the vector changes by $(\Delta\mathbf{x} \cdot \nabla)\mathbf{v}dt$.

the notation D/Dt is used in some older texts for the convective derivative d/dt.) The geometrical meaning of the fluid derivative can be understood from Fig. 14.2. Denote by $\Delta\mathbf{x}(t)$ the vector connecting two points $\mathcal{P}$ and $\mathcal{Q}$ that are moving with the fluid. Then the convective derivative $d\Delta\mathbf{x}/dt$ must equal the relative velocity of these two points, namely $(\Delta\mathbf{x} \cdot \nabla)\mathbf{v}$. In other words, the fluid derivative of $\Delta\mathbf{x}$ vanishes

$$\frac{D\Delta\mathbf{x}}{Dt} = 0 \; . \tag{14.7}$$

More generally, *the fluid derivative of any vector can be understood as its rate of change relative to a vector moving with the fluid.*

14.2.2 Barotropic, Inviscid Flows: Vortex Lines Frozen Into Fluid

In order to understand the vorticity evolution law (14.6) physically, let us specialize to a barotropic $[P = P(\rho)]$, inviscid ($\nu = 0$) fluid flow. (This is the kind of flow that usually occurs in the Earth's atmosphere and oceans, well away from solid boundaries.) Then the last two terms in Eq. (14.6) vanish, leaving

$$\frac{D\boldsymbol{\omega}}{Dt} = -\boldsymbol{\omega}\nabla \cdot \mathbf{v} \; . \tag{14.8}$$

Equation (14.8) says that the vorticity has a fluid derivative parallel to itself. In this sense we can speak of the vortex lines as being *frozen* into the moving fluid.

We can actually make the fluid derivative vanish by substituting $\nabla \cdot \mathbf{v} = -\rho^{-1}d\rho/dt$ (the equation of mass conservation) into Eq. (14.8); the result is

$$\boxed{\frac{D}{Dt}\left(\frac{\boldsymbol{\omega}}{\rho}\right) = 0 \quad \text{for barotropic, inviscid flow.}} \tag{14.9}$$

Therefore, the quantity $\boldsymbol{\omega}/\rho$ evolves according to the same equation as the separation $\Delta\mathbf{x}$ of two points in the fluid. To see what this implies, consider a small cylindrical fluid element whose symmetry axis is parallel to $\boldsymbol{\omega}$ (Fig. 14.3). Denote its vectorial length by $\Delta\mathbf{x}$ and its vectorial cross sectional area by $\Delta\boldsymbol{\Sigma}$. Then since $\boldsymbol{\omega}/\rho$ points along $\Delta\mathbf{x}$ and both are
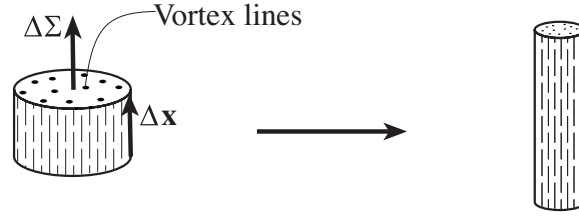
Fig. 14.3: Simple demonstration of the kinematics of vorticity propagation in a barotropic, inviscid flow. A short, thick cylindrical fluid element with generators parallel to the local vorticity gets deformed, by the flow, into a long, slender cylinder. By virtue of Eq. (14.9), we can think of the vortex lines as being convected with the fluid, with no creation of new lines or destruction of old ones, so that the number of vortex lines passing through the cylinder (through its end surface $\Delta\boldsymbol{\Sigma}$) remains constant.

frozen into the fluid, it must be that $\boldsymbol{\omega}/\rho = \text{constant} \times \Delta\mathbf{x}$. Therefore, the fluid element's conserved mass is $\Delta M = \rho\Delta\mathbf{x}\cdot\Delta\boldsymbol{\Sigma} = \text{constant} \times \boldsymbol{\omega}\cdot\Delta\boldsymbol{\Sigma}$, so $\boldsymbol{\omega}\cdot\Delta\boldsymbol{\Sigma}$ is conserved as the cylindrical fluid element moves and deforms. We thereby conclude that *the fluid's vortex lines, with number per unit area proportional to $|\boldsymbol{\omega}|$, are convected by our barotropic, inviscid fluid, without having to be created or destroyed.*

   If the flow is not only barotropic and inviscid, but also incompressible (as it usually is to high accuracy in the oceans and atmosphere), then Eqs. (14.8) and (14.9) say that $D\boldsymbol{\omega}/Dt = 0$. Suppose, in addition, that the flow is 2-dimensional (as it commonly is to moderate accuracy when averaged over transverse scales large compared to the thickness of the atmosphere and oceans), so $\mathbf{v}$ is in the x and y directions and independent of z. This means that $\boldsymbol{\omega} = \omega\mathbf{e}_z$ and we can regard the vorticity as the scalar ω. Then Eq. (14.5) with $(\boldsymbol{\omega}\cdot\boldsymbol{\nabla})\mathbf{v} = 0$ implies that the vorticity obeys the simple propagation law

$$\frac{d\omega}{dt} = 0 \; . \tag{14.10}$$

Thus, *in a 2-dimensional, incompressible, barotropic, inviscid flow, the vorticity is convected conservatively, just like entropy per unit mass in an adiabatic fluid.*

14.2.3   Tornados

A particularly graphic illustration of the behavior of vorticity is provided by a tornado. Tornadoes in North America are most commonly formed at a front where cold, dry air from the north meets warm, moist air from the south, and huge, cumulo-nimbus thunderclouds form. A strong updraft of the warm, moist air creates rotational motion about a horizontal axis, and updraft of the central part of the rotation axis itself makes it somewhat vertical. A low pressure vortical core is created at the center of this spinning fluid, and the spinning region lengthens under the action of up and down drafts. Now, consider this in the context of vorticity propagation. As the air, to first approximation, is incompressible, a lengthening of the spinning region's vortex lines corresponds to a reduction in the cross section and a strengthening of the vorticity. This, in turn, corresponds to an increase in the tornado's circulatory speeds. (Speeds in excess of 450 km/hr have been reported.) If and when the

tornado touches down to the ground and its very-low-pressure core passes over the walls and roof of a building, the far larger, normal atmospheric pressure inside the building can cause the building to explode. Further details are explored in Exs. 13.9 and 14.2.

14.2.4   Kelvin's Theorem

Intimately related to vorticity is a quantity called the *circulation* Γ; it is defined as the line integral of the velocity around a closed curve ∂S lying in the fluid

$$\boxed{\Gamma \equiv \int_{\partial S} \mathbf{v} \cdot d\mathbf{x}}, \tag{14.11a}$$

and it can be regarded as a property of the closed curve ∂S. We can invoke Stokes' theorem to convert this circulation into a surface integral of the vorticity passing through a surface S bounded by ∂S:

$$\boxed{\Gamma = \int_{S} \boldsymbol{\omega} \cdot d\boldsymbol{\Sigma}}. \tag{14.11b}$$

[Note, though, that Eq. (14.11b) is only valid if the area bounded by the contour is simply connected; in particular, if the area enclosed contains a solid body, Eq. (14.11b) may fail.] Equation (14.11b) says that the circulation Γ is the flux of vorticity through S, or equivalently it is proportional to the number of vortex lines passing through S. Circulation is thus the fluid counterpart of magnetic flux.

Kelvin's theorem tells us the rate of change of the circulation associated with a particular contour ∂S that is attached to the moving fluid. Let us evaluate this directly using the convective derivative of Γ. We do this by differentiating the two vector quantities inside the integral (14.11a):

$$\begin{aligned} \frac{d\Gamma}{dt} &= \int_{\partial S} \frac{d\mathbf{v}}{dt} \cdot d\mathbf{x} + \int_{\partial S} \mathbf{v} \cdot d\left(\frac{d\mathbf{x}}{dt}\right) \\ &= -\int_{\partial S} \frac{\boldsymbol{\nabla}P}{\rho} \cdot d\mathbf{x} - \int_{\partial S} \boldsymbol{\nabla}\Phi \cdot d\mathbf{x} + \nu \int_{\partial S} (\nabla^2 \mathbf{v}) \cdot d\mathbf{x} + \int_{\partial S} d\frac{1}{2}v^2, \end{aligned} \tag{14.12}$$

where we have used the Navier Stokes equation (14.2) with ν = constant. The second and fourth terms on the right hand side of Eq. (14.12) vanish around a closed curve and the first can be rewritten in different notation to give

$$\boxed{\frac{d\Gamma}{dt} = -\int_{\partial S} \frac{dP}{\rho} + \nu \int_{\partial S} (\nabla^2 \mathbf{v}) \cdot d\mathbf{x}}. \tag{14.13}$$

This is Kelvin's theorem for the evolution of circulation. In a rotating reference frame it must be augmented by the integral of the Coriolis acceleration $-2\boldsymbol{\Omega} \times \mathbf{v}$ around the closed curve ∂S, and if the fluid is electrically conducting and possesses a magnetic field it must be augmented by the integral of the Lorentz force per unit mass $\mathbf{J} \times \mathbf{B}/\rho$ around ∂S.

If the fluid is barotropic, $P = P(\rho)$, and the effects of viscosity are negligible (and the coordinates are inertial and there is no magnetic field and electric current), then the right hand side of Eq. (14.13) vanishes, and Kelvin's theorem takes the simple form

$$\boxed{\frac{d\Gamma}{dt} = 0 \quad \text{for barotropic, inviscid flow.}} \tag{14.14}$$

This is the global version of our result that the circulation $\boldsymbol{\omega} \cdot \Delta\boldsymbol{\Sigma}$ of an infinitesimal fluid element is conserved.

The qualitative content of Kelvin's theorem is that vorticity in a fluid is long-lived. Once a fluid develops some circulation, this circulation will persist, unchanged, unless and until the fluid can develop some shear stress, either directly through viscous action, or indirectly through the $\boldsymbol{\nabla} P \times \boldsymbol{\nabla} \rho$ term or a Coriolis or Lorentz force term in Eq. (14.3).

14.2.5   Diffusion of Vortex Lines

Next, consider the action of viscous stresses on an existing vorticity field. For an incompressible, barotropic fluid with nonnegligible viscosity, the vorticity evolution law (14.6) says

$$\boxed{\frac{D\boldsymbol{\omega}}{Dt} = \nu\nabla^2\boldsymbol{\omega} \quad \text{for incompressible, barotropic fluid.}} \tag{14.15}$$

This is a "convective" vectorial diffusion equation: the viscous term $\nu\nabla^2\boldsymbol{\omega}$ causes the vortex lines to diffuse through the moving fluid. When viscosity is negligible, the vortex lines are frozen into the flow. When viscosity is significant and no boundaries impede the vorticity's diffusion, the vorticity spreads away from its source to occupy an area $\sim \nu t$ in the moving fluid after a time t [Ex. 14.3]. The kinematic viscosity, therefore, not only has the dimensions of a diffusion coefficient, it actually controls the diffusion of vortex lines relative to the moving fluid.

As a simple example of the spreading of vortex lines, consider an infinite plate moving parallel to itself relative to a fluid at rest. Let us transform to the rest frame of the plate [Fig. 14.4a] so the fluid moves past it. Suppose that at time $t = 0$ the velocity has only a component v_x parallel to the plate, which depends solely on the distance y from the plate, so the flow is translation invariant in the x direction; then it will continue always to be translation invariant. Suppose further that, at $t = 0$, v_x is constant except in a thin boundary layer near the plate, where it drops rapidly to 0 at $y = 0$ (as it must, because of the plate's "no-slip" boundary condition); cf. Fig. 14.4b. As the flow is a function only of y (and t), and $\mathbf{v}$ and $\boldsymbol{\omega}$ point in directions orthogonal to $\mathbf{e}_y$, in this flow the fluid derivative D/Dt [Eq. (14.5)] reduces to $\partial/\partial t$ and the convective diffusion equation (14.15) becomes an ordinary scalar diffusion equation, $\partial\omega_z/\partial t = \nu\nabla^2\omega_z$ for the only nonzero component of the vorticity. Let the initial thickness of the boundary layer, at time $t = 0$, be $\delta(0)$. Then, our experience with the diffusion equation [e.g., Exs. 3.16 and 6.3] tells us that the viscosity will diffuse through the fluid, under the action of viscous stress, and as a result, the boundary-layer thickness will increase with time as

$$\delta(t) \sim (\nu t)^{\frac{1}{2}} \quad \text{for} \quad t \gtrsim \delta(0)^2/\nu ; \tag{14.16}$$

see Fig. 14.4(c).
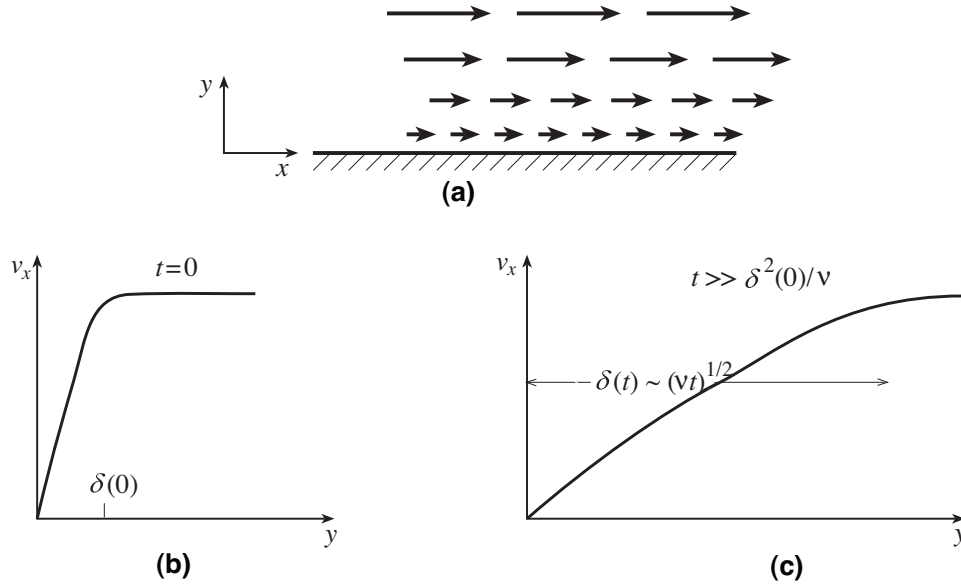
Fig. 14.4: A simple shear layer that is translation invariant along the flow direction, x. Vorticity diffuses away from the static plate at $y = 0$, under the action of viscous torques, in much the same way that heat diffuses away from a heated surface.

## 14.2.6 Sources of Vorticity.

Having discussed how vorticity is conserved in simple inviscid flows and how it diffuses away under the action of viscosity, we must now consider its sources. The most important source is a solid surface. When fluid suddenly encounters a solid surface like the leading edge of an airplane wing, intermolecular forces act to decelerate the fluid very rapidly in a thin boundary layer along the surface. This introduces circulation and consequently vorticity into the flow, where none existed before; and that vorticity then diffuses into the bulk flow, thickening the boundary layer (Sec. 14.4 below).

If the fluid is non-barotropic, then pressure gradients can also create vorticity, as described by the second term on the right hand side of our vorticity evolution law (14.6), $-\boldsymbol{\nabla} P \times \boldsymbol{\nabla} \rho / \rho^2$. Physically what happens is that, when the surfaces of constant pressure (*isobars*) do not coincide with the surfaces of constant density (*isochors*), then the net pressure force on a small fluid element does not pass through its center of mass, and the pressure therefore exerts a torque on the fluid element, introducing some rotational motion and vorticity. (See Figure 14.5.) Non-barotropic pressure gradients can therefore create vorticity within the body of the fluid. Note that as the vortex lines must be continuous, any fresh ones that are created within the fluid must be created as loops that expand from a point or a line.

There are *three other common sources of vorticity* in fluid dynamics: *Coriolis forces* (when one's reference frame is rotating rigidly), *curving shock fronts* (when the fluid speed is supersonic) and *Lorentz forces* (when the fluid is electrically conducting). We shall discuss these in Sec. 14.5 and Chaps 17 and 19, respectively.

****
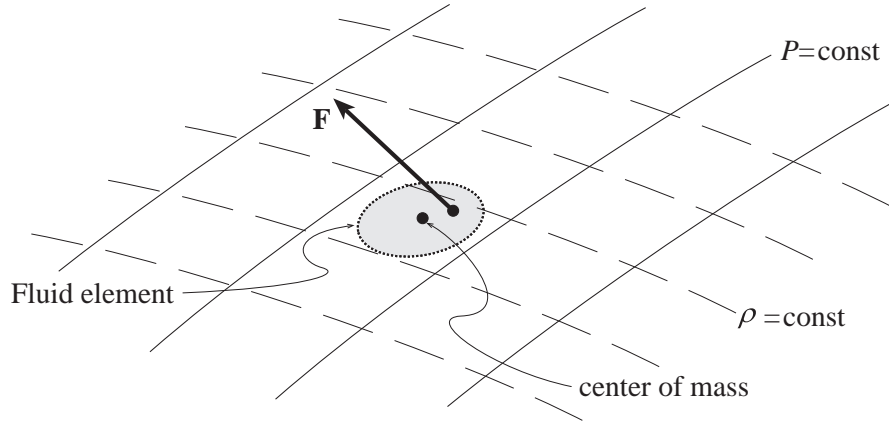
Fig. 14.5: Mechanical explanation for the creation of vorticity in a non-barotropic fluid. The net pressure gradient force **F** acting on a small fluid element is normal to the isobars (solid lines) and does not pass through the center of mass of the element; thereby a torque is produced.

EXERCISES

Exercise 14.1 *Practice: Vorticity and incompressibility*
Sketch the streamlines for the following stationary two dimensional flows, determine if the fluid is compressible, and evaluate its vorticity. The coordinates are Cartesian in (a) and (b), and are circular polar with orthonormal bases $\{\mathbf{e}_\varpi, \mathbf{e}_\phi\}$ in (c) and (d).

(a) $v_x = 2xy, \quad v_y = x^2$.

(b) $v_x = x^2, \quad v_y = -2xy$

(c) $v_\varpi = 0, \quad v_\phi = \varpi$

(d) $v_\varpi = 0, \quad v_\phi = \varpi^{-1}$.

Exercise 14.2 *Problem: Tornado*

(a) Figure 14.6 shows photographs of two particularly destructive tornados and one waterspout (a tornado sucking water). For the tornados the wind speeds near the ground are particularly high: about 450 km / hr. Estimate the wind speeds at the top, where the tornados merge with the clouds. For the water spout, the wind speed near the water is about 150 km/hr. Estimate the wind speed at the top

(b) Estimate the air pressure in the cores of these tornados and water spout, in atmospheres. [Hint: Use Crocco's Theorem, Ex. 13.9.]

Exercise 14.3 ***Example: Vorticity Used to Solve for Flow Details*
At time $t = 0$, a two-dimensional barotropic flow has a velocity field, in circular polar coordinates, $\mathbf{v} = (j/\varpi)\mathbf{e}_\phi$ (Fig. 14.1b) and, correspondingly, its vorticity is $\boldsymbol{\omega} = 2\pi j\delta(x)\delta(y)\mathbf{e}_z$. In this exercise you will solve for the full details of the subsequent evolution of the flow.

Fig. 14.6: Phtographs of two destructive tornados and a waterspout. [Credits: Left – Greg Stumpf (NOAA), Center – Tribune Weekly Chronicle, Right – Joseph Golden (NOAA).

(a) Solve the vorticity evolution equation (14.6) to determine the vorticity as a function of time. From your solution, show that the area in which the vorticity is concentrated at time t is $A \sim \nu t$, and show that the vorticity is becoming smoothed out — it is evolving toward a state of uniform vorticity, where the viscosity will no longer have any influence.

(b) From your computed vorticity, plus circular symmetry, compute the velocity field as a function of time.

(c) From the Navier Stokes equation, or equally well from Crocco's theorem, compute the evolution of the pressure distribution $P(\varpi, t)$.

Remark: This exercise illustrates a frequent phenonenon in fluid mechanics: The pressure adjusts itself to whatever it needs to be, to accommodate the flow. One can often solve for it in the end, after having worked out other details. This happens here because, when one takes the curl of the Navier Stokes equation for a barotropic fluid (which we did to get our evolution equation for vorticity), the pressure drops out, i.e., it decouples from the evolution equation for vorticity and thence velocity.

Exercise 14.4 ***Example: Joukowski's Theorem for the Lift on an Airplane Wing*
When an appropriately curved airfoil (e.g., an airplane wing) is introduced into a steady flow of air, the air has to flow faster along the upper surface than the lower surface and this can create a lifting force (Fig. 14.7.) In this situation, compressibility and gravity are usually unimportant for the flow. Show that the pressure difference across the airfoil is given approximately by

$$\Delta P = \frac{1}{2}\rho\Delta(v^2) = \rho v \Delta v .$$

Hence show that the lift exerted by the air on an airfoil of length L is given approximately by

$$\boxed{F_L = L\int \Delta P d\mathbf{x} = \rho v L \Gamma} ,$$
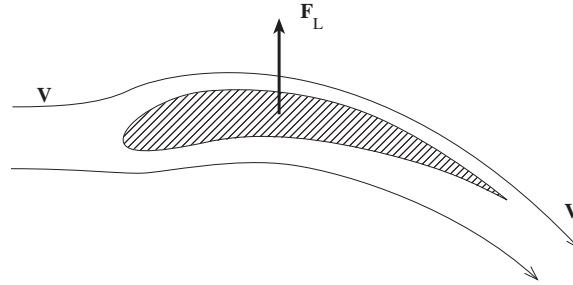
Fig. 14.7: Flow around an airfoil.

where Γ is the circulation around the airfoil. This is known as *Joukowski's theorem*. Interpret this result in terms of the conservation of linear momentum, and sketch the overall flow pattern.

Exercise 14.5 ****Example: Rotating Superfluids*
Certain fluids at low temperature undergo a phase transition to a superfluid state. A good example is ^{4}He for which the transition temperature is 2.2K. As a superfluid has no viscosity, it cannot develop vorticity. How then can it rotate? The answer (e.g. Feynman 1972) is that not all the fluid is in a superfluid state; some of it is normal and can have vorticity. When the fluid rotates, all the vorticity is concentrated within microscopic vortex cores of normal fluid that are parallel to the rotation axis and have quantized circulations $\Gamma = h/m$, where m is the mass of the atoms and h is Planck's constant. The fluid external to these vortex cores is irrotational (has vanishing vorticity). These normal fluid vortices may interact with the walls of the container.

(a) Explain, using a diagram, how the vorticity of the macroscopic velocity field, averaged over many vortex cores, is twice the mean angular velocity of the fluid.

(b) Make an order of magnitude estimate of the spacing between these vortex cores in a beaker of superfluid helium on a turntable rotating at 10 rpm.

(c) Repeat this estimate for a millisecond neutron star, which mostly comprises superfluid neutron pairs at the density of nuclear matter and spins with a period of order a millisecond. (The mass of the star is roughly 3×10^{30}kg.)

****

14.3   Low-Reynolds-Number Flow – Stokes Flow and Sedimentation

In the last chapter, we defined the Reynolds number Re to be the product of the characteristic speed V and lengthscale a of a flow divided by its kinematic viscosity $\nu = \eta/\rho$: $R \equiv$

Va/ν. The significance of the Reynolds number follows from the fact that, in the Navier Stokes equation (14.2), the ratio of the magnitude of the inertial term $|(\mathbf{v} \cdot \boldsymbol{\nabla})\mathbf{v}|$ to the viscous acceleration, $|\nu\nabla^2\mathbf{v}|$ is approximately equal to Re. Therefore, when $R \ll 1$, the inertial acceleration can often be ignored and the velocity field is determined by balancing the pressure gradient against the viscous stress. The velocity then scales linearly with the magnitude of the pressure gradient and vanishes when the pressure gradient vanishes. This has the amusing consequence that a low Reynolds number flow driven by a solid object moving through a fluid at rest is effectively reversible; if the motion of the object is reversed, then the fluid elements will return almost to their original positions.

From the magnitudes of viscosities of real fluids (Table 13.2 on page 13.36), it follows that the low Reynolds number limit is appropriate either for very small scale flows (e.g. the motion of micro-organisms) or for very viscous large scale fluids (e.g. the earth's mantle).

14.3.1   Motivation: Climate Change

A very important example of a small-scale flow arises in the issue of the degree to which cooling of the Earth due to volcanic explosions can mitigate global warming.

The context is concern about anthropogenic (man-made) climate change. The Earth's atmosphere is a subtle and fragile protector of the environment that allows life to flourish. Especially worrisome is the increase in atmospheric carbon dioxide — by nearly 25% over the past fifty years to a mass of 3×10^{15} kg. As an important greenhouse gas, carbon dioxide traps solar radiation. Increases in its concentration are contributing to the observed increase in mean surface temperature, the rise of sea levels and the release of oceanic carbon dioxide with potential runaway consequences.

These effects are partially mitigated by volcanos like Krakatoa, which exploded in 1883, releasing roughly 200 Megatons or $\sim 10^{18}$ J of energy and nearly 10^{14} kg of aerosol particles (soot etc.), of which $\sim 10^{12}$ kg was raised into the the stratosphere, where much of it remained for several years. These micron-sized particles absorb light with roughly their geometrical cross section. As the area of the earth's surface is roughly 7×10^{14}m^2, and the density of the particles is roughly 2000kg m^{-3}, 10^{12}kg of aerosols is sufficient to blot out the sun. More specifically, the micron-sized particles absorb solar optical and ultraviolet radiation while remaining reasonably transparent to infra-red radiation escaping from the earth's surface. The result is a noticeable global cooling of the earth for as long as the soot remains suspended in the atmosphere.[3]

A key issue in assessing how our environment is likely to change over the next century is how long the small particles of soot etc. will remain in the atmosphere after volcanic explosions, i.e. their rate of sedimentation. This is a problem in low Reynolds' number flow. We shall model the sedimentation by computing the speed at which a spherical soot particle falls through quiescent air when the Reynolds number is small. The speed is governed by a balance between the downward force of gravity and the speed-dependent upward drag force of the air. We shall compute this speed by first evaluating the force of the air on the moving

---

[3]Similar effects would follow the explosion of nuclear weapons in a major nuclear war according to Turco et al (1983), a phenomenon that they dubbed "nuclear winter".

particle ignoring gravity, and then, at the end of the calculation, inserting the influence of gravity.

14.3.2 Stokes Flow

We model the soot particle as a sphere of radius a. The low-Reynolds-number flow of a viscous fluid past such a sphere is known as *Stokes flow*. We will calculate the flow's velocity field, and then from it, the force of the fluid on the sphere. (This calculation also finds application in the famous Millikan oil drop experiment.)

It is easiest to tackle this problem in the frame of the sphere, where the flow is stationary (time-independent). We seek a solution to the Navier Stokes equation in which the flow velocity, $\mathbf{v}(\mathbf{x})$, tends to a constant value $\mathbf{V}$ (the velocity of the sphere through the fluid), at large distances from the sphere's center. We presume the asymptotic flow velocity $\mathbf{V}$ to be highly subsonic so the flow is effectively incompressible, $\boldsymbol{\nabla} \cdot \mathbf{v} = 0$.
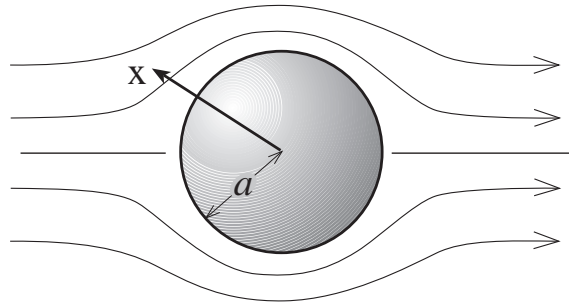
Fig. 14.8: Stokes flow around a sphere.

We define the Reynolds number for this flow by Re $= \rho V a / \eta = V a / \nu$. As this is assumed small, in the Navier Stokes equation (14.2) we can ignore the inertial term, which is $O(V \Delta v / a)$, in comparison with the viscous term, which is $O(\eta \Delta v / a^2 \rho)$; here $\Delta v \sim V$ is the total velocity variation. The time-independent Navier Stokes equation (14.2) can thus be well-approximated by $\boldsymbol{\nabla} P = \rho \boldsymbol{g} + \eta \nabla^2 \mathbf{v}$. The uniform gravitational force density $\rho \boldsymbol{g}$ is obviously balanced by a uniform pressure gradient (hydrostatic equilibrium). Removing these uniform terms from both sides of the equation, we get

$$\boldsymbol{\nabla} P = \eta \nabla^2 \mathbf{v} , \tag{14.17}$$

where $\boldsymbol{\nabla} P$ is now just the nonuniform part of the pressure gradient required to balance the viscous force density. The full details of the flow are governed by this force-balance equation, the flow's incompressibility

$$\boldsymbol{\nabla} \cdot \mathbf{v} = 0 , \tag{14.18}$$

and the boundary conditions $\mathbf{v} = 0$ at $r = a$ and $\mathbf{v} \to \mathbf{V}$ at $r \to \infty$.

From force balance (14.17) we infer that in order of magnitude the difference between the fluid's pressure on the front of the sphere and that on the back is $\Delta P \sim \eta V / a$. We also expect a viscous drag stress along the sphere's sides of magnitude $T_{r\theta} \sim \eta V / a$, where V / a is the magnitude of the shear. These two stresses, acting on the sphere's surface area $\sim a^2$ will

produce a net drag force $F \sim \eta V a$. Our goal is to verify this order of magnitude estimate, compute the force more accurately, then balance this force against gravity (adjusted for the much smaller Archimedes buoyancy force produced by the uniform part of the pressure gradient), and thereby infer the speed of fall V of a soot particle.

For a highly accurate analysis of the flow, we could write the full solution as a perturbation expansion in powers of the Reynolds number Re. We shall compute only the leading term in this expansion; the next term, which corrects for inertial effects, will be smaller than our solution by a factor $O(\mathrm{Re})$.

Our solution to this classic problem is based on some general principles that ought to be familiar from other areas of physics. First, we observe that the quantities in which we are interested are the pressure P, the velocity $\mathbf{v}$ and the vorticity $\boldsymbol{\omega}$, a scalar, a polar vector and an axial vector, respectively, and at first order in the Reynolds number they should be linear in $\mathbf{V}$. The only scalar we can form, linear in $\mathbf{V}$, is $\mathbf{V} \cdot \mathbf{x}$ so we expect the variable part of the pressure to be proportional to this combination. For the polar-vector velocity we have two choices, a part $\propto \mathbf{V}$ and a part $\propto (\mathbf{V} \cdot \mathbf{x})\mathbf{x}$; both terms are present. Finally for the axial-vector vorticity, our only option is a term $\propto \mathbf{V} \times \mathbf{x}$. We shall use these combinations below.

Now take the divergence of Eq. (14.17), and conclude that the pressure must satisfy Laplace's equation, $\nabla^2 P = 0$. The solution should be axisymmetric about $\mathbf{V}$, and we know that axisymmetric solutions to Laplace's equation that decay as $r \to \infty$ can be expanded as a sum over Legendre polynomials, $\sum_{\ell=0}^{\infty} P_\ell(\mu)/r^{\ell+1}$, where μ is the cosine of the angle θ between $\mathbf{V}$ and $\mathbf{x}$, and r is $|\mathbf{x}|$. Since $P \propto \mathbf{V} \cdot \mathbf{x}$, the dipolar, $\ell = 1$ term [for which $P_1(\mu) = \mu = \mathbf{V} \cdot \mathbf{x}/(Vr)$] is all we need; the higher-order polynomials will be higher-order in $\mathbf{V}$ and thus must arise at higher orders of the Reynolds-number expansion. We therefore write

$$P = P_\infty + \frac{k\eta(\mathbf{V} \cdot \mathbf{x})a}{r^3} + \dots . \tag{14.19}$$

Here k is a numerical constant which we must determine, we have introduced a factor η to make k dimensionless, and P_∞ is the pressure far from the sphere.

Next consider the vorticity. Since it is proportional to $\mathbf{V} \times \mathbf{x}$ and cannot depend in any other way on $\mathbf{V}$, it must be expressible as

$$\boldsymbol{\omega} = \frac{\mathbf{V} \times \mathbf{x}}{a^2} f(r/a) . \tag{14.20}$$

The factor a appears in the denominator to make the unknown function $f(\xi)$ dimensionless. We determine this unknown function by rewriting Eq. (14.17) in the form

$$\boldsymbol{\nabla} P = -\eta \boldsymbol{\nabla} \times \boldsymbol{\omega} \tag{14.21}$$

[which we can do because $\boldsymbol{\nabla} \times \boldsymbol{\omega} = -\nabla^2 \mathbf{v} + \boldsymbol{\nabla}(\boldsymbol{\nabla} \cdot \mathbf{v})$, and $\boldsymbol{\nabla} \cdot \mathbf{v} = 0$], and then inserting Eqs. (14.19) amd (14.20) into (14.21) to obtain $f(\xi) = k\xi^{-3}$, whence

$$\boldsymbol{\omega} = \frac{k(\mathbf{V} \times \mathbf{x})a}{r^3} \tag{14.22}$$

Now, Eq. (14.22) for the vorticity looks familiar. It has the form of the Biot-Savart law for the magnetic field from a current element. We can therefore write down immediately a formula for its associated "vector potential", which in this case is the velocity:

$$\mathbf{v}(\mathbf{x}) = \frac{ka\mathbf{V}}{r} + \boldsymbol{\nabla}\psi \ . \tag{14.23}$$

The addition of the $\boldsymbol{\nabla}\psi$ term corresponds to the familiar gauge freedom in defining the vector potential. However in the case of fluid dynamics, where the velocity is a directly observable quantity, the choice of the scalar ψ is fixed by the boundary conditions instead of being free. As ψ is a scalar linear in $\mathbf{V}$, it must be expressible in terms of a second dimensionless function $g(\xi)$ as

$$\psi = g(r/a)\mathbf{V} \cdot \mathbf{x} \ . \tag{14.24}$$

Next we recall that the flow is incompressible, i.e. $\boldsymbol{\nabla} \cdot \mathbf{v} = 0$. Substituting Eq. (14.24) into Eq. (14.23) and setting the divergence expressed in spherical polar coordinates to zero, we obtain an ordinary differential equation for g

$$\frac{d^2g}{d\xi^2} + \frac{4}{\xi}\frac{dg}{d\xi} - \frac{k}{\xi^3} = 0. \tag{14.25}$$

This has the solution,

$$g(\xi) = A - \frac{k}{2\xi} + \frac{B}{\xi^3} \ , \tag{14.26}$$

where A and B are integration constants. As $\mathbf{v} \to \mathbf{V}$ far from the sphere, the constant $A = 1$. The constants B, k can be found by imposing the boundary condition $\mathbf{v} = 0$ for $r = a$. We thereby obtain $B = -1/4, k = -3/2$ and after substituting into Eq. (14.23) we obtain for the velocity field

$$\mathbf{v} = \left[1 - \frac{3}{4}\left(\frac{a}{r}\right) - \frac{1}{4}\left(\frac{a}{r}\right)^3\right]\mathbf{V} - \frac{3}{4}\left(\frac{a}{r}\right)^3\left[1 - \left(\frac{a}{r}\right)^2\right]\frac{(\mathbf{V} \cdot \mathbf{x})\mathbf{x}}{a^2} \ . \tag{14.27}$$

The associated pressure and vorticity, from Eqs. (14.19) and (14.22), are given by

$$P = P_\infty - \frac{3\eta a(\mathbf{V} \cdot \mathbf{x})}{2r^3} \ ,$$
$$\boldsymbol{\omega} = \frac{3a(\mathbf{x} \times \mathbf{V})}{2r^3}. \tag{14.28}$$

The pressure is seen to be largest on the upstream hemisphere as expected. However, the vorticity, which points in the direction of $\mathbf{e}_\phi$, is seen to be symmetric between the front and the back of the sphere. This is because, under our low Reynolds number approximation, we are neglecting the advection of vorticity by the velocity field and only retaining the diffusive term. Vorticity is generated on the front surface of the sphere at a rate $\nu\omega_{\phi,r} = 3\nu V \sin\theta/a^2$ per unit length and diffuses into the surrounding flow; then, after the flow passes the sphere's equator, the vorticity diffuses back inward and is absorbed onto the sphere's back face. An analysis that includes higher orders in the Reynolds number would show that not all of the vorticity is reabsorbed; a small portion is left in the fluid, downstream from the sphere.

We have been able to obtain a simple solution for low Reynolds number flow past a sphere. Although closed form solutions like this are not common, the methods that were used to derive it are of widespread applicability. Let us recall them. First, we approximated the equation of motion by omitting the sub-dominant inertial term and invoked a symmetry argument. We used our knowledge of elementary electrostatics to write the pressure in the form (14.19). We then invoked a second symmetry argument to solve for the vorticity and drew upon another analogy with electromagnetic theory to derive a differential equation for the velocity field which was solved subject to the no-slip boundary condition on the surface of the sphere.

Having obtained a solution for the velocity field and pressure, it is instructive to re-examine our approximations. The first point to notice is that the velocity perturbation, given by Eq. (14.27) dies off slowly, inversely proportional to distance r from the sphere. This implies that, in order for our solution to be valid, the region through which the sphere is moving must be much larger than the sphere; otherwise the boundary conditions at $r \to \infty$ have to be modified. This is not a concern for a soot particle in the atmosphere. A second, related point is that, if we compare the sizes of the inertial term (which we neglected) and the pressure gradient (which we kept) in the full Navier Stokes equation, we find

$$|(\mathbf{v} \cdot \nabla)\mathbf{v}| \sim \frac{V^2 a}{r^2} \;, \quad \left| \frac{\boldsymbol{\nabla} P}{\rho} \right| \sim \frac{\eta a V}{\rho r^3} \;. \tag{14.29}$$

At $r = a$ their ratio is $Va\rho/\eta = Va/\nu$, which is the (small) Reynolds number. However, at a distance $r \sim \eta/\rho V = a/R$ from the sphere's center, the inertial term becomes comparable to the pressure term. Correspondingly, in order to improve on our zero order solution, we must perform a second expansion at large r including inertial effects and then match it asymptotically to a near zone expansion. This technique of *matched asymptotic expansions* is a very powerful and general way of finding approximate solutions valid over a wide range of length scales where the dominant physics changes from one scale to the next. We shall present an explicit example of such a matched asymptotic expansion in Sec. 16.5.3.

Let us return to the problem that motivated this calculation: estimating the drag force on the sphere. This can be computed by integrating the stress tensor $\mathbf{T} = P\mathbf{g} - 2\eta\boldsymbol{\sigma}$ over the surface of the sphere. If we introduce a local orthonormal basis, $\mathbf{e}_r, \mathbf{e}_\theta, \mathbf{e}_\phi$ with polar axis ($\theta = 0$) along the flow direction $\mathbf{V}$, then we readily see that the only non-zero viscous contribution to the surface stress tensor is $T_{r\theta} = T_{\theta r} = \eta \partial v_\theta / \partial r$. The net resistive force along the direction of the velocity is then given by

$$\begin{aligned} F &= \int_{r=a} \frac{d\boldsymbol{\Sigma} \cdot \mathbf{T} \cdot \mathbf{V}}{V} \\ &= -\int_0^{2\pi} 2\pi a^2 \sin\theta d\theta \left[-P_\infty \cos\theta + \frac{3\eta V \cos^2\theta}{2a} + \frac{3\eta V \sin^2\theta}{2a} \right] \;. \end{aligned} \tag{14.30}$$

The integrals are elementary; they give for the total resistive force

$$\boxed{\mathbf{F} = -6\pi\eta a\mathbf{V}} \;. \tag{14.31}$$

This is Stokes' Law for the drag force in low Reynolds number flow. Two-thirds of the force comes from the viscous stress and one third from the pressure.

14.3.3   Sedimentation Rate

In order to compute the sedimentation rate of soot particles relative to the air we must restore gravity to our analysis. We can do so by restoring to the Navier Stokes equation the uniform pressure gradient and balancing gravitational term that we removed just before Eq. (14.17). Gravity and the buoyancy (Archimedes) force from the uniform pressure gradient exert a net downward force $(4\pi a^3/3)(\rho_s - \rho)\boldsymbol{g}$ on the soot particle, which must balance the upward resistive force (14.31). Here $\rho_s \sim 2000$kg m^{-3} is the density of soot and $\rho \sim 1$ kg m^{-3} is the far smaller (and here negligible) density of air. Equating these forces, we obtain

$$V = \frac{2\rho_s a^2 g_e}{9\eta} \tag{14.32}$$

Now, the kinematic viscosity of air at sea level is, according to Table 13.2, $\nu \sim 10^{-5}$ m^{2}s^{-1} and the density is $\rho_a \sim 1$kg m^{-3}, so the coefficient of viscosity is $\eta = \rho_a \nu \sim 10^{-5}$kg m^{-1}s^{-1}. This viscosity is proportional to the square root of temperature and independent of the density [cf. Eq. (12.68)]; however, the temperature does not vary by more than about 25 per cent through the atmosphere, so for order of magnitude calculations we can use its value at sea level. Substituting the above values into (14.32), we obtain an equilibrium sedimentation speed

$$V \sim 0.5(a/1\mu)^2 \text{mm s}^{-1} \tag{14.33}$$

We should also, for self-consistency, estimate the Reynolds number; it is

$$\text{Re} \sim \frac{2aV}{\eta} \sim 10^{-4} \left(\frac{a}{1\mu}\right)^3 . \tag{14.34}$$

Our analysis is therefore only likely to be adequate for particles of radius $a \lesssim 10\mu$.

The sedimentation speed (14.33) is much smaller than wind speeds in the upper atmosphere $v_{\text{wind}} \sim 30$m s^{-1}. However, as the stratosphere is reasonably stratified, the net vertical motion due to the winds is quite small and so we can estimate the settling time by dividing the stratosphere's height ~ 30km by the speed (14.33) to obtain

$$t_{\text{settle}} \sim 6 \times 10^7 \left(\frac{a}{1\mu}\right)^{-2} \text{s} \sim 2 \left(\frac{a}{1\mu}\right)^{-2} \text{months.} \tag{14.35}$$

This calculation is a simple model for more serious and complex analyses of sedimentation after volcanic eruptions, and the resulting mitigation of global warming. Of course, huge volcanic eruptions are rare, so no matter the result of reliable future analyses, we cannot count on volcanos to save humanity from runaway global warming.

****

EXERCISES

Exercise 14.6 *Problem: Oseen's Paradox*
Consider low Reynolds number flow past an infinite cylinder and try to repeat the analysis we used for a sphere to obtain an order of magnitude estimate for the drag force per unit length. Do you see any difficulty, especially concerning the analog of Eq. (14.29)?

Exercise 14.7 *Problem: Viscosity of the Earth's mantle.*
Episodic glaciation subjects the earth's crust to loading and unloading by ice. The last major
ice age was 10,000 years ago, and the subsequent unloading produces a non-tidal contribution
to the acceleration of the earth's rotation rate of order

$$\frac{|\mathbf{\Omega}|}{|\dot{\mathbf{\Omega}}|} \simeq 6 \times 10^{11}\mathrm{yr} \; ,$$

detectable from observing the positions of distant stars. Corresponding changes in the earth's
oblateness produce a decrease in the rate of nodal line regression of the geodetic satellite
LAGEOS.

(a) Estimate the speed with which the polar regions (treated as spherical caps of radius
~ 1000km) are rebounding now. Do you think the speed was much greater in the past?

(b) Geological evidence suggests that a particular glaciated region of radius about 1000km
sank in ~ 3000yr during the last ice age. By treating this as a low Reynolds number
viscous flow, make an estimate of the coefficient of viscosity for the mantle.

****************************

14.4 High-Reynolds-Number Flow – Laminar Boundary Layers

As we have described, flow near a solid surface creates vorticity and, consequently, the
velocity field near the surface cannot be derived from a scalar potential, $\mathbf{v} = \mathbf{\nabla}\psi$. However,
if the Reynolds number is high, then the vorticity may be localized within a thin boundary
layer adjacent to the surface, as in Fig. 14.4 above; and the flow may be very nearly of
potential form $\mathbf{v} = \mathbf{\nabla}\psi$ outside that boundary layer. In this section we shall use the
equations of hydrodynamics to model the flow in the simplest example of such a boundary
layer: that formed when a long, thin plate is placed in a steady, uniform flow $V\mathbf{e}_x$ with its
surface parallel to the flow (Fig. 14.9).

If the plate is not too long (see caption of Fig. 14.9), then the flow will be *laminar*, i.e.
steady and two-dimensional—a function only of the distances x along the plate's length and
y perpendicular to the plate (both being measured from an origin at the plate's front). We
assume the flow to be very subsonic, so it can be regarded as incompressible. As the viscous
stress decelerates the fluid close to the plate, it must therefore be deflected away from the
plate to avoid accumulating, thereby producing a small y component of velocity along with
the larger x component. As the velocity is uniform well away from the plate, the pressure
is constant outside the boundary layer. We use this to motivate the approximation that
P is also constant within the boundary layer. After solving for the flow, we will check the
self-consistency of this *ansatz* (guess). With $P = $ constant and the flow stationary, only the
inertial and viscous terms remain in the Navier Stokes equation (14.2):

$$(\mathbf{v} \cdot \nabla)\mathbf{v} \simeq \nu\nabla^2\mathbf{v} \; . \tag{14.36}$$
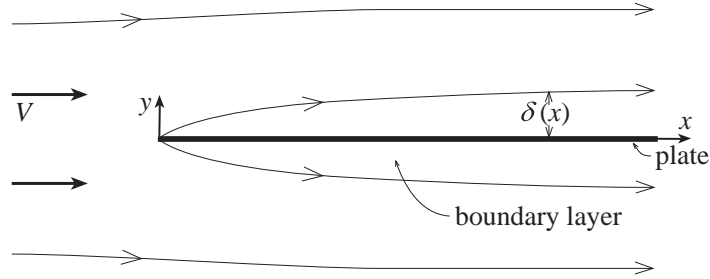
Fig. 14.9: Laminar boundary layer formed by a long, thin plate in a flow with asymptotic speed V. The length ℓ of the plate must give a Reynolds number $\mathrm{Re}_\ell \equiv V\ell/\nu$ in the range $10 \lesssim \mathrm{Re}_\ell \lesssim 10^6$; if Re_ℓ is much less than 10, the plate will be in or near the regime of low Reynolds number flow (Sec. 14.3 above), and the boundary layer will be so thick everywhere that our analysis will fail. If Re_ℓ is much larger than 10^6, then at sufficiently great distances x down the plate ($\mathrm{Re}_x = Vx/\nu \gtrsim 10^6$), a portion of the boundary layer will become unstable and its simple laminar structure will be destroyed; see Chap. 14.

This equation must be solved in conjunction with $\boldsymbol{\nabla} \cdot \mathbf{v} = 0$ and the boundary conditions $\mathbf{v} \to V\mathbf{e}_x$ as $y \to \infty$ and $\mathbf{v} \to 0$ as $y \to 0$.

The fluid first encounters the no-slip boundary condition at the front of the plate, $x = y = 0$. The flow there abruptly decelerates to vanishing velocity, creating a sharp velocity gradient that contains a sharp spike of vorticity. This is the birth of the boundary layer.
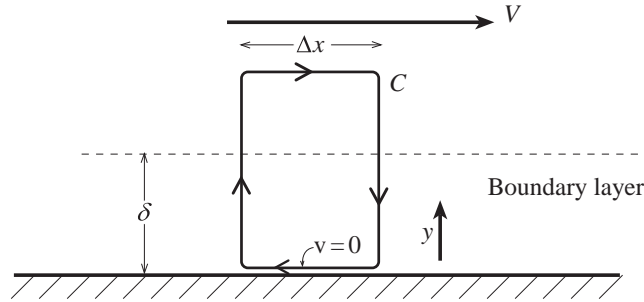
Fig. 14.10: A rectangle C used in showing that a boundary layer's circulation per unit length $\Gamma_C/\Delta x$ is equal to the flow speed V just above the boundary layer.

Further downstream, the total flux of vorticity inside the rectangle C of Fig. 14.31, $\int \boldsymbol{\omega} \cdot d\boldsymbol{\Sigma}$, is equal to the circulation $\Gamma_C = \int_C \mathbf{v} \cdot d\mathbf{x}$ around C. The flow velocity is zero on the bottom leg of C and it is (very nearly) orthogonal to C on the vertical legs, so the only nonzero contribution is from the top leg, which gives $\Gamma_C = V\Delta x$. Therefore, the circulation per unit length (flux of vorticity per unit length $\Gamma_C/\Delta x$) is V everywhere along the plate. This means that there is no new vorticity acquired and none lost, after the initial spike at the front of the plate.

As the fluid flows on down the plate, from $x = 0$ to larger x, the spike of vorticity, created at the plate's leading edge, gradually diffuses outward from the wall into the flow, thickening the boundary layer.

Let us compute, in order of magnitude, the boundary layer's thickness $\delta(x)$ as a function

of distance x down the plate. Incompressibility, $\boldsymbol{\nabla} \cdot \mathbf{v} = 0$, implies that $v_y \sim v_x \delta/x$. Using this to estimate the relative magnitudes of the various terms in the x component of the force balance equation (14.36), we see that the dominant inertial term (left hand side) is $\sim V^2/x$ and the dominant viscous term (right hand side) is $\sim \nu V/\delta^2$. We therefore obtain the estimate $\delta \sim \sqrt{\nu x/V}$. This motivates us to define the function

$$\boxed{\delta(x) \equiv \left(\frac{\nu x}{V}\right)^{1/2}}. \tag{14.37}$$

for use in our quantitative analysis. Our analysis will reveal that the actual thickness of the boundary layer is several times larger than this $\delta(x)$.

Equation (14.37) shows that the boundary layer has a parabolic shape, $y \sim \delta(x) = \sqrt{\nu x/V}$. To keep our analysis manageable, we shall confine ourselves to the region, not too close to the front of the plate, where the layer is thin, $\delta \ll x$, and the velocity is nearly parallel to the plate, $v_y \sim (\delta/x)v_x \ll v_x$.

14.4.1 Similarity Solution for Velocity Field

To proceed further, we use a technique of widespread applicability in fluid mechanics: we make a *similarity anszatz* (guess), whose validity we will verify near the end of the calculation. We suppose that, once the boundary layer has become thin ($\delta \ll x$), the cross sectional shape of the flow is independent of distance x down the plate (it is "similar" at all x). Stated more precisely, we assume that $v_x(x, y)$ (which has magnitude $\sim V$) and $(x/\delta)v_y$ (which also has magnitude $\sim V$) are functions only of the single transverse, dimensionless variable

$$\boxed{\xi = \frac{y}{\delta(x)} = y\sqrt{\frac{V}{\nu x}}}. \tag{14.38}$$

Our task, then, is to compute $\mathbf{v}(\xi)$ subject to the boundary conditions $\mathbf{v} = 0$ at $\xi = 0$, and $\mathbf{v} = V\mathbf{e}_x$ at $\xi \gg 1$. We do so with the aid of a second, very useful calculational device. Recall that any vector field [$\mathbf{v}(\mathbf{x})$ in our case] can be expressed as the sum of the gradient of a scalar potential and the curl of a vector potential, $\mathbf{v} = \boldsymbol{\nabla}\psi + \boldsymbol{\nabla} \times \mathbf{A}$. If our flow were irrotational $\boldsymbol{\omega} = 0$, we would need only $\boldsymbol{\nabla}\psi$, but it is not; the vorticity in the boundary layer is large. On the other hand, to high accuracy the flow is incompressible, $\theta = \boldsymbol{\nabla} \cdot \mathbf{v} = 0$, which means we need only the vector potential, $\mathbf{v} = \boldsymbol{\nabla} \times \mathbf{A}$; and because the flow is two dimensional (depends only on x and y and has $\mathbf{v}$ pointing only in the x and y directions), the vector potential need only have a z component, $\mathbf{A} = A_z\mathbf{e}_z$. We denote its nonvanishing component by $A_z \equiv \zeta(x, y)$ and give it the name *stream function*, since it governs how the laminar flow streams. In terms of the stream function, the relation $\mathbf{v} = \boldsymbol{\nabla} \times A$ takes the simple form

$$\boxed{v_x = \frac{\partial \zeta}{\partial y}, \quad v_y = -\frac{\partial \zeta}{\partial x}}. \tag{14.39}$$

This, automatically, satisfies $\boldsymbol{\nabla} \cdot \mathbf{v} = 0$. Notice that $\mathbf{v} \cdot \boldsymbol{\nabla}\zeta = v_x\partial\zeta/\partial x + v_y\partial\zeta/\partial y = -v_xv_y + v_yv_x = 0$. Thus, *the stream function is constant along streamlines*.

Since the stream function varies on the lengthscale δ, in order to produce a velocity field with magnitude $\sim V$, it must have magnitude $\sim V\delta$. This motivates us to *guess* that it has the functional form

$$\zeta = V\delta(x)f(\xi) \,, \tag{14.40}$$

where $f(\xi)$ is some dimensionless function of order unity. This will be a good guess if, when inserted into Eq. (14.39), it produces a self-similar flow, i.e. one with v_x and $(x/\delta)v_y$ depending only on ξ. Indeed, inserting Eq. (14.40) into Eq. (14.39), we obtain

$$v_x = Vf' \,, \quad v_y = \frac{\delta(x)}{2x}V(\xi f' - f) \,, \tag{14.41a}$$

where the prime means $d/d\xi$. This has the desired self-similar form.

By inserting these self-similar v_x and v_y into the x component of the force-balance equation (14.36), we obtain a non-linear third order differential equation for $f(\xi)$

$$\frac{d^3 f}{d\xi^3} + \frac{f}{2}\frac{d^2 f}{d\xi^2} = 0 \tag{14.41b}$$

The fact that this equation involves x and y only in the combination $\xi = y\sqrt{V/\nu x}$ confirms that our self-similar anszatz was a good one. Equation (14.41b) must be solved subject to the boundary condition that the velocity vanish at the surface and approach V as $y \to \infty$ ($\xi \to \infty$); i.e. [cf. Eqs. (14.41a)] that

$$f(0) = f'(0) = 0 \,, \quad f'(\infty) = 1 \,. \tag{14.41c}$$
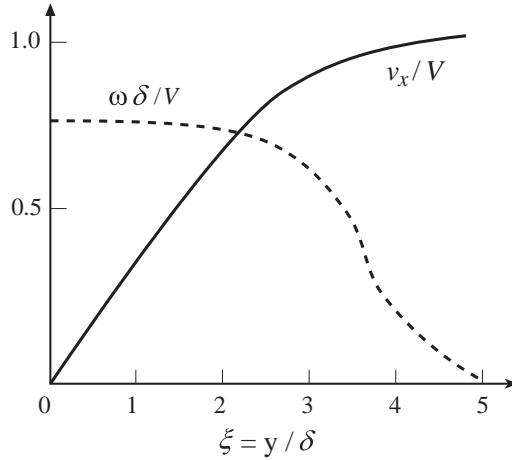
Fig. 14.11: Scaled velocity profile $v_x/V = f'(\xi)$ (solid line) for a laminar boundary layer as a function of scaled perpendicular distance $\xi = y/\delta$. Note that the flow speed is 90 per cent of V at a distance of 3δ from the surface and so δ is a good measure of the thickness of the boundary layer. Also shown is the scaled vorticity profile $\omega\delta/V$. [These figures are hand-sketched; a more accurate numerically generated solution will be provided in future version of this chapter.]

Not surprisingly, Eq. (14.41b) does not admit an analytic solution. However, it is simple to compute a numerical solution with the boundary conditions (14.41c). The result for $v_x/V = f'(\xi)$ is shown in Fig. 14.11. This solution, the *Blasius profile*, has qualitatively the form we expected: the velocity v_x rises from 0 to V in a smooth manner as one moves outward from the plate, achieving a sizable fraction of V at a distance several times larger than $\delta(x)$.

This Blasius profile is our first example of a common procedure in fluid dynamics: taking account of a natural scaling in the problem to make a self-similar anzatz and thereby transform the partial differential fluid equations into ordinary differential equations. Solutions of this type are known as *similarity solutions.*

The motivation for using similarity solutions is obvious. The non-linear partial differential equations of fluid dynamics are much harder to solve, even numerically, than ordinary differential equations. Elementary similarity solutions are especially appropriate for problems where there is no characteristic length or timescale associated with the relevant physical quantities except those explicitly involving the spatial and temporal coordinates. Large Reynolds number flow past a large plate has a useful similarity solution, whereas flow with $\text{Re}_\ell \sim 1$, where the size of the plate is clearly a significant scale in the problem, does not. We shall encounter more examples of similarity solutions in the following chapters.

Now that we have a solution for the flow, we must examine a key approximation that underlies it: constancy of the pressure P. To do this, we begin with the y component of the force-balance equation (14.36) (a component that we never used explicitly in our analysis). The inertial and viscous terms are both $O(V^2\delta/x^2)$, so if we re-instate a term $-\boldsymbol{\nabla}P/\rho \sim -\Delta P/\rho\delta$, it can be no larger than the other two terms. From this we estimate that the pressure difference across the boundary layer is $\Delta P \lesssim \rho V^2 \delta^2/x^2$. Using this estimate in the x component of force balance (14.36) (the component on which our analysis was based), we verify that the pressure gradient term is smaller than those we kept by a factor $\lesssim \delta^2/x^2 \ll 1$. For this reason, *when the boundary layer is thin we can, indeed, neglect pressure gradients across it when computing its structure from longitudinal force balance.*

It is of interest to compute the total drag force exerted on the plate. Letting ℓ be the plate's length and $w \gg \ell$ be its width, and noting that the plate has two sides, the drag force produced by the viscous stress acting on the plate's surface is

$$F = 2\int T_{xy}^{\text{vis}}dxdz = 2\int (-2\eta\sigma_{xy})dxdz = 2w\int_0^\ell \rho\nu\left(\frac{\partial v_x}{\partial y}\right)_{y=0} dx \ . \tag{14.42}$$

Inserting $\partial v_x/\partial y = (V/\delta)f''(0) = V\sqrt{V/\nu x}f''(0)$ from Eq. (14.41a), and performing the integral, we obtain

$$\boxed{F = \frac{1}{2}\rho V^2 \times (2\ell w) \times C_D} \ , \tag{14.43}$$

where

$$\boxed{C_D = 4f''(0)R_\ell^{-1/2}} \ . \tag{14.44}$$

Here we have introduced an often-used notation for expressing the drag force of a fluid on a solid body: we have written it as half the incoming fluid's kinetic stress ρV^2, times the surface

area of the body $2\ell w$ on which the drag force acts, times a dimensionless drag coefficient C_D, and we have expressed the drag coefficient in terms of the Reynolds number

$$\boxed{\mathrm{Re}_\ell = \frac{V\ell}{\nu}} \tag{14.45}$$

formed from the body's relevant dimension, ℓ, and the speed and viscosity of the incoming fluid.

From Fig. 14.11, we estimate that $f''(0) \simeq 0.3$ (an accurate numerical value is 0.332), and so $C_D \simeq 1.328 R_\ell^{-1/2}$. Note that the drag coefficient decreases as the viscosity decreases and the Reynolds number increases. However, as we shall discuss in Chap. 15, this model breaks down for very large Reynolds numbers $\mathrm{Re}_\ell \gtrsim 10^6$ because a portion of the boundary layer becomes turbulent.

14.4.2 Vorticity Profile

It is illuminating to consider the structure of the boundary layer in terms of its vorticity. Since the flow is two-dimensional with velocity $\mathbf{v} = \boldsymbol{\nabla} \times (\zeta \mathbf{e}_z)$, its vorticity is $\boldsymbol{\omega} = \boldsymbol{\nabla} \times \boldsymbol{\nabla} \times (\zeta \mathbf{e}_z) = -\nabla^2(\zeta \mathbf{e}_z)$, which has as its only nonzero component

$$\omega \equiv \omega_z = -\nabla^2 \zeta \simeq -\frac{V}{\delta} f''(\xi) \ . \tag{14.46}$$

This vorticity is exhibited in Fig. 14.11 above.

From Eq. (14.41b), we observe that the gradient of vorticity vanishes at the plate. This means that the vorticity is not diffusing out of the plate's surface. Neither is it being convected away from the plate's surface, as the perpendicular velocity vanishes there. This confirms what we already learned from Fig. 14.10: the flux per unit length of vorticity is conserved along the plate, once it has been created as a spike at the plate's leading edge.

If we transform into a frame moving with an intermediate speed $\sim V/2$, and measure time t since passing the leading edge, the vorticity will diffuse a distance $\sim (\nu t)^{1/2} \sim (\nu x/V)^{1/2} = \delta(x)$ away from the surface after time t; see the discussion of vorticity diffusion in Sec. 14.2.5. This exhibits the connection between that diffusion discussion and the similarity solution for the boundary layer in this section.
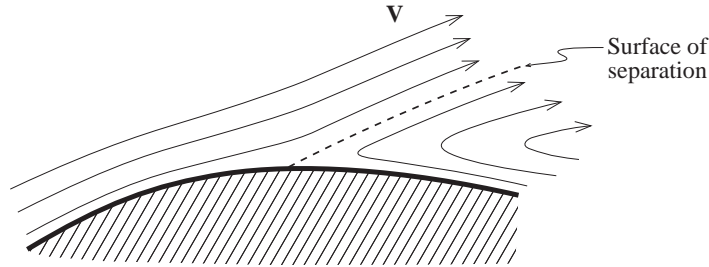
Fig. 14.12: Separation of a boundary layer in the presence of an adverse pressure gradient.

14.4.3 Separation

Next consider flow past a non-planar surface, e.g. an aircraft wing. In this case, there in general will be a pressure gradient along the boundary layer, which cannot be ignored in contrast to the pressure gradient across the boundary layer. If the pressure decreases along the flow, the flow will accelerate and more vorticity will be created at the surface and will diffuse away from the surface. However, if there is an "adverse" pressure gradient and the flow decelerates, then negative vorticity must be created at the wall. For a sufficiently adverse gradient, the negative vorticity gets so strong that it cannot diffuse fast enough into and through the boundary layer to maintain a simple boundary-layer-type flow. Instead, the boundary layer *separates* from the surface, as shown in Fig. 14.12, and a backward-flow is generated beyond the separation point by the negative vorticity. This phenomenon can occur on an aircraft when the wings' angle of attack (i.e. the inclination of the wings to the horizontal) is too great. An unfavorable pressure gradient develops on the upper wing surfaces, the flow separates and the plane stalls. The designers of wings make great effort to prevent this, as we shall discuss briefly in the next chapter.

****

EXERCISES

Exercise 14.8 *Example: Potential Flow around a Cylinder (D'Alembert's Paradox)*
Consider stationary incompressible flow around a cylinder of radius a with sufficiently large Reynolds number that viscosity may be ignored except in a thin boundary layer which is assumed to extend all the way around the cylinder. The velocity is assumed to have the uniform value **V** at large distances from the cylinder.

(a) Show that the velocity field outside the boundary layer may be derived from a scalar potential ψ which satisfies Laplace's equation, $\nabla^2 \psi = 0$.

(b) Write down suitable boundary conditions for ψ.

(c) Write the velocity potential in the form

$$\psi = \mathbf{V} \cdot \mathbf{x} + f(\mathbf{x})$$

and solve for f. Sketch the streamlines and equipotentials.

(d) Next use Bernoulli's equation to compute the pressure distribution over the surface and the net drag force given by this solution. Does your drag force seem reasonable? It did not seem reasonable to d'Alembert in 1752, and it came to be called *d'Alembert's paradox*.

(e) Finally, consider the effect of the pressure distribution on the boundary layer. How do you think this will make the real flow be different from the potential solution? How will the drag change?

Exercise 14.9 *Problem: Reynolds Numbers*
Estimate the Reynolds numbers for the following flows. Make sketches of the flow fields pointing out any salient features.

(a) A hang glider in flight.

(b) Planckton in the ocean.

(c) A physicist waving her hands.

Exercise 14.10 *Problem: Fluid Dynamical Scaling*
An auto manufacturer wishes to reduce the drag force on a new model by changing its design. She does this by building a one eighth scale model and putting it into a wind tunnel. How fast must the air travel in the wind tunnel to simulate the flow at 60 mph on the road?

[Remark: This is our first example of "scaling" relations in fluid dynamics, a powerful concept that we shall develop and explore in later chapters.]

Exercise 14.11 *Example: Stationary Laminar Flow down a Long Pipe*
Fluid flows down a long cylindrical pipe with length b much larger than radius a, from a reservoir maintained at pressure P_0 which connects to the pipe at $x = 0$, to a free end at large x, where the pressure is negligible. In this problem, we try to understand the velocity field $v_x(\varpi, x)$ as a function of radius ϖ and distance x down the pipe, for a given "discharge" (i.e. mass flow per unit time) $\dot{M}$. We assume that the Reynolds number is small enough for the flow to be treated as laminar all the way down the pipe.

(a) Close to the entrance of the pipe (small x), the boundary layer will be very thin and the velocity will be nearly independent of radius. What will be the fluid velocity outside the boundary layer in terms of its density and $\dot{M}$?

(b) How far must the fluid travel along the pipe before the vorticity diffuses into the center of the flow and the boundary layer becomes as thick as the radius? An order of magnitude calculation is adequate and you may assume that the pipe is much longer than your estimate.

(c) At a sufficiently great distance down the pipe, the profile will cease evolving with x and settle down into the Poiseuille form derived in Sec. 13.7.6, with the discharge $\dot{M}$ given by the Poiseuille formula. Sketch how the volocity profile changes along the pipe, from the entrance to this final Poiseuille region.

(d) Outline a procedure for computing the discharge in a long pipe of arbitrary cross section.

****

14.5 Nearly Rigidly Rotating Flows — Earth's Atmosphere and Oceans

One often encounters, in Nature, fluids that are nearly rigidly rotating, i.e. fluids with a nearly uniform distribution of vorticity. The Earth's oceans and atmosphere are important examples, where the rotation is forced by the underlying rotation of the Earth. Such rotating fluids are best analyzed in a rotating reference frame, in which the unperturbed fluid is at rest and the perturbations are influenced by Coriolis forces, resulting in surprising phenomena. We shall explore some of these phenomena in this section.

14.5.1 Equations of Fluid Dynamics in a Rotating Reference Frame

As a foundation for this exploration, we wish to transform the Navier Stokes equation from the inertial frame in which it was derived to a uniformly rotating frame: the mean rest frame of the flows we shall study.

We begin by observing that the Navier Stokes equation has the same form as Newton's second law for particle motion:

$$\frac{d\mathbf{v}}{dt} = \mathbf{f},\tag{14.47}$$

where the force per unit mass is $\mathbf{f} = -\boldsymbol{\nabla}P/\rho - \boldsymbol{\nabla}\Phi + \nu\nabla^2\mathbf{v}$. We transform to a frame rotating with uniform angular velocity $\boldsymbol{\Omega}$ by adding "fictitious" Coriolis and centrifugal accelerations, given respectively by $-2\boldsymbol{\Omega}\times\mathbf{v}$ and $-\boldsymbol{\Omega}\times(\boldsymbol{\Omega}\times\mathbf{x})$, and expressing the force $\mathbf{f}$ in rotating coordinates. The fluid velocity transforms as

$$\mathbf{v} \to \mathbf{v} + \boldsymbol{\Omega}\times\mathbf{x}.\tag{14.48}$$

It is straightforward to verify that this transformation leaves the expression for the viscous acceleration, $\nu\nabla^2\mathbf{v}$, unchanged. Therefore the expression for the force is unchanged, and the Navier Stokes equation in rotating coordinates becomes

$$\frac{d\mathbf{v}}{dt} = -\frac{\boldsymbol{\nabla}P}{\rho} - \boldsymbol{\nabla}\Phi + \nu\nabla^2\mathbf{v} - 2\boldsymbol{\Omega}\times\mathbf{v} - \boldsymbol{\Omega}\times(\boldsymbol{\Omega}\times\mathbf{x})\,.\tag{14.49}$$

Now, the centrifugal acceleration $-\boldsymbol{\Omega}\times(\boldsymbol{\Omega}\times\mathbf{x})$ can be expressed as the gradient of a centrifugal potential, $\boldsymbol{\nabla}[\frac{1}{2}(\boldsymbol{\Omega}\times\mathbf{x})^2] = \boldsymbol{\nabla}[\frac{1}{2}(\Omega\varpi)^2]$, where ϖ is distance from the rotation axis. (The location of the rotation axis is actually arbitrary, aside from the requirement that it be parallel to $\boldsymbol{\Omega}$; see Box 14.3.) For simplicity, we shall confine ourselves to an incompressible fluid so that ρ is constant. This allows us to define an *effective pressure*

$$\boxed{P' = P + \rho\left[\Phi - \frac{1}{2}(\boldsymbol{\Omega}\times\mathbf{x})^2\right]}\tag{14.50}$$

that includes the combined effects of the real pressure, gravity and the centrifugal force. In terms of P' the Navier Stokes equation in the rotating frame becomes

$$\boxed{\frac{d\mathbf{v}}{dt} = -\frac{\boldsymbol{\nabla}P'}{\rho} + \nu\nabla^2\mathbf{v} - 2\boldsymbol{\Omega}\times\mathbf{v}}\,.\tag{14.51a}$$

The quantity P' will be constant if the fluid is at rest in the rotating frame, $\mathbf{v} = 0$, in contrast to the true pressure P which does have a gradient. Equation (14.51a) is the most useful form for the Navier Stokes equation in a rotating frame. For incompressible (very subsonic) flows we augment it by the incompressibility condition $\boldsymbol{\nabla} \cdot \mathbf{v} = 0$, which is left unchanged by the transformation (14.48) to a rotating reference frame:

$$\boxed{\boldsymbol{\nabla} \cdot \mathbf{v} = 0} \ . \tag{14.51b}$$

It should be evident from Eq. (14.51a) that two dimensionless numbers characterize rotating fluids. The first is the *Rossby number*,

$$\boxed{\mathrm{Ro} = \frac{V}{\Omega L}} \ , \tag{14.52}$$

where V is a characteristic velocity of the flow relative to the rotating frame and L is a characteristic length. Ro measures the relative strength of the inertial acceleration and the Coriolis acceleration:

$$\boxed{\mathrm{Ro} \sim \frac{|(\mathbf{v} \cdot \boldsymbol{\nabla})\mathbf{v}|}{|2\boldsymbol{\Omega} \times \mathbf{v}|} \sim \frac{\text{inertial force}}{\text{Coriolis force}}} \ . \tag{14.53}$$

The second dimensionless number is the *Ekman number*,

$$\boxed{\mathrm{Ek} = \frac{\nu}{\Omega L^2}} \ ; \ , \tag{14.54}$$

which similarly measures the relative strengths of the viscous and Coriolis accelerations:

$$\boxed{\mathrm{Ek} \sim \frac{|\nu \nabla^2 \mathbf{v}|}{|2\boldsymbol{\Omega} \times \mathbf{v}|} \sim \frac{\text{viscous force}}{\text{Coriolis force}}} \ . \tag{14.55}$$

Notice that $\mathrm{Ro}/\mathrm{Ek} = \mathrm{Re}$ is the Reynolds' number.

The three traditional examples of rotating flows are large-scale storms and other weather patterns on the rotating earth, deep currents in the earth's oceans, and water in a stirred teacup.

For a typical storm, the wind speed might be $L \sim 25$ mph ~ 10 m s^{-1}, and a characteristic length scale might be $L \sim 1000$ km. The effective angular velocity at a temperate latitude is (see Box 14.3) $\Omega_\star = \Omega_\oplus \sin 45° \sim 10^{-4}$ rad s^{-1}, where $\Omega_\oplus$ is the Earth's angular velocity. As the air's kinematic viscosity is $\nu \sim 10^{-5}$ m^2 s^{-1}, we find that Ro ~ 0.1 and Ek $\sim 10^{-13}$. This tells us immediately that Coriolis forces are important but not totally dominant, compared to inertial forces, in controlling the weather, and that viscous forces are unimportant except in very thin boundary layers.

For deep ocean currents such as the gulf stream, V ranges from ~ 0.01 to ~ 1 m s^{-1}, so we use $V \sim 0.1$ m s^{-1}, and lengthscales are $L \sim 1000$ km, so Ro $\sim 10^{-3}$ and Ek $\sim 10^{-14}$. Thus, Coriolis accelerations are far more important than inertial forces, and viscous forces are important only in very thin boundary layers.

Box 14.3
Arbitrariness of Rotation Axis; Ω for Atmospheric and Oceanic Flows

In this box we elucidate two issues:

Arbitrariness of Rotation Axis. Imagine yourself on the rotation axis $\mathbf{x} = 0$ of a rigidly rotating flow. All fluid elements circulate around you with angular velocity $\boldsymbol{\Omega}$. Now move perpendicular to the rotation axis, to a new location $\mathbf{x} = \mathbf{a}$, and ride with the flow there. All other fluid elements will still rotate around you with angular velocity $\boldsymbol{\Omega}$! The only way you can know you have moved (if all fluid elements look identical) is that you will now experience a centrifugal force $\boldsymbol{\Omega} \times (\boldsymbol{\Omega} \times \mathbf{a})$.

This shows up mathematically in the rotating-frame Navier Stokes equation (14.49). When we set $\mathbf{x} = \mathbf{x}_{\text{new}} - \mathbf{a}$, the only term that changes is the centrigual force; it becomes $-\boldsymbol{\Omega} \times (\boldsymbol{\Omega} \times \mathbf{x}_{\text{new}}) + \boldsymbol{\Omega} \times (\boldsymbol{\Omega} \times \mathbf{a})$. If we absorb the new, constant, centrifugal term $\boldsymbol{\Omega} \times (\boldsymbol{\Omega} \times \mathbf{a})$ into the gravitational acceleration $\boldsymbol{g} = -\boldsymbol{\nabla}\Phi$, then the Navier Stokes equation is completely unchanged. In this sense, the choice of rotation axis is arbitrary.

Ω *for Large-Scale Flows in the Earth's Atmosphere and Oceans* For large-scale flows in the earth's atmosphere and oceans (e.g. storms), the rotation of the unperturbed fluid is that due to rotation of the earth. One might think that this means we should take, as the angular velocity $\boldsymbol{\Omega}$ in the Coriolis term of the Navier Stokes equation (14.51a), the earth's angular velocity $\boldsymbol{\Omega}_\oplus$. Not so. The atmosphere and ocean are so thin vertically that vertical motions cannot achieve small Rossby numbers; i.e. Coriolis forces are unimportant for vertical motions. Correspondingly, the only component of the Earth's angular velocity $\boldsymbol{\Omega}_\oplus$ that is important for Coriolis forces is that which couples horizontal flows to horizontal flows: the vertical component $\Omega_* = \Omega_\oplus \sin(\text{latitute})$. (A similar situation occurs for a Foucault pendulum). Thus, in the Coriolis term of the Navier Stokes equation we must set $\boldsymbol{\Omega} = \Omega_* \mathbf{e}_z = \Omega_\oplus \sin(\text{latitude})\mathbf{e}_z$, where $\mathbf{e}_z$ is the vertical unit vector. By contrast, in the centrifugal potential $\frac{1}{2}(\boldsymbol{\Omega} \times \mathbf{x})^2$, $\boldsymbol{\Omega}$ remains the full angular velocity of the Earth, $\boldsymbol{\Omega}_\oplus$ — unless we absorb a portion of it into the gravitational potential as when we change rotation axes, in which case we can use $\boldsymbol{\Omega} = \Omega_* \mathbf{e}_z$ in the centrifugal potential.

For water stirred in a teacup (with parameters typical of many flows in the laboratory), $L \sim 10$ cm, $\Omega \sim V/L \sim 10$ rad s^{-1} and $\nu \sim 10^{-6}$ m^2 s^{-1} giving Ro ~ 1, Ek $\sim 10^{-5}$. Coriolis and inertial forces are comparable in this case, and viscous forces again are confined to boundary layers, but the layers are much thicker relative to the bulk flow than in the atmospheric and oceanic cases.

Notice that for all these flows — atmospheric, oceanic, and tea cup — the (effective) rotation axis is vertical, i.e. $\boldsymbol{\Omega}$ is vertically directed (cf. Box 14.3). This will be the case for all nearly rigidly rotating flows considered in this chapter.

14.5.2 Geostrophic Flows

Stationary flows $\partial \mathbf{v}/\partial t = 0$ in which both the Rossby and Ekman numbers are small (i.e. with Coriolis forces big compared to inertial and viscous forces) are called *geostrophic*, even in the laboratory. Geostrophic flow is confined to the bulk of the fluid, well away from all boundary layers, since viscosity will become important in those layers. For such geostrophic flows, the Navier Stokes equation (14.51a) reduces to

$$\boxed{2\boldsymbol{\Omega} \times \mathbf{v} = -\frac{\boldsymbol{\nabla} P'}{\rho} \quad \text{for geostrophic flow.}} \tag{14.56}$$

This equation says that the velocity $\mathbf{v}$ (measured in the rotating frame) is orthogonal to the body force $\boldsymbol{\nabla} P'$, which drives it. Correspondingly, the streamlines are perpendicular to the gradient of the generalized pressure; i.e. they lie in the surfaces of constant P'.

An example of geostrophic flow is the motion of atmospheric winds around a low pressure region or *depression*. [Since $P' = P + \rho(\Phi - \frac{1}{2}\Omega\varpi^2)$, when the actual pressure P goes up or down at some fixed location, P' goes up or down by the same amount, so a depression of P' is a depression of P.] The geostrophic equation (14.56) tells us that such winds must be counter-clockwise in the northern hemisphere as seen from a satellite, and clockwise in the southern hemisphere. For a flow with speed $v \sim 10$ m s^{-1} around a ~ 1000 km depression, the drop in effective pressure at the depression's center is $\Delta P' = \Delta P \sim 1$ kPa ~ 10 mbar ~ 0.01 atmosphere ~ 0.3 inches of mercury. Around a high-pressure region winds will circulate in the opposite direction.

It is here that we can see the power of introducing the effective pressure P'. In the case of atmospheric and oceanic flows, the true pressure P changes significantly vertically, and the pressure scale height is generally much shorter than the horizontal length scale. However, the effective pressure will be almost constant vertically, any small variation being responsible for minor updrafts and downdrafts which we generally ignore when describing the wind or current flow pattern. It is the horizontal pressure gradients which are responsible for driving the flow. When pressures are quoted, they must therefore be referred to some reference equipotential surface, $\Phi - \frac{1}{2}(\boldsymbol{\Omega} \times \mathbf{x})^2 =$ constant. The convenient one to use is the equipotential associated with the surface of the ocean, usually called "mean sea level". This is the pressure that appears on a meteorological map.

14.5.3 Taylor-Proudman Theorem

There is a simple theorem due to Taylor and Proudman which simplifies the description of three dimensional, geostrophic flows. Take the curl of Eq. (14.56) and use $\boldsymbol{\nabla} \cdot \mathbf{v} = 0$ for incompressible flow; the result is

$$\boxed{(\boldsymbol{\Omega} \cdot \nabla)\mathbf{v} = 0} \,. \tag{14.57}$$

Thus, there can be no vertical gradient (gradient along $\boldsymbol{\Omega}$) of the velocity under geostrophic conditions. This result provides a good illustration of the stiffness of vortex lines: The vortex lines associated with the rigid rotation $\boldsymbol{\Omega}$ are frozen into the fluid under geostrophic conditions (where other contributions to the vorticity are small), and they refuse to be bent. The simplest demonstration of this is the Taylor column of Fig. 14.13.

It is easy to see that *any* vertically constant, divergence-free velocity field $\mathbf{v}(x, y)$ can be a solution to the geostrophic equation (14.56). The generalized pressure P' can be adjusted to make it a solution (cf. the discussion of pressure adjusting itself to whatever the flow requires, in Ex. 14.3). However, one must keep in mind that to guarantee it is also a true (approximate) solution of the full Navier Stokes equation (14.51a), its Rossby and Ekman numbers must be $\ll 1$.

View from Above   Side View
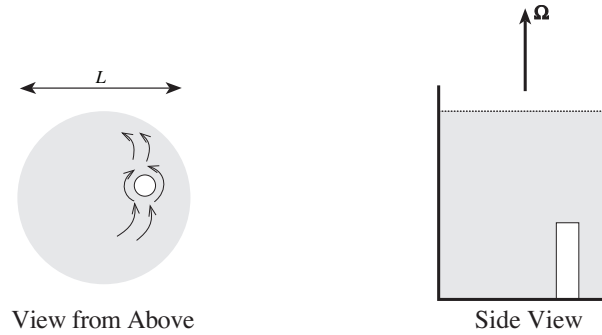
Fig. 14.13: Taylor Column. A solid cylinder (white) is placed in a large container of water which is then spun up on a turntable to a high enough angular velocity Ω that the Ekman number is small, $\mathrm{Ek} = \nu/\Omega L^2 \ll 1$. A slow, steady flow relative to the cylinder is then induced. (The flow's velocity $\mathbf{v}$ in the rotating frame must be small enough to keep the Rossby number $\mathrm{Ro} = v/\Omega L \ll 1$.) The water in the bottom half of the container flows around the cylinder. The water in the top half does the same as if there were an invisible cylinder present. This is an illustration of the Taylor-Proudman theorem which states that there can be no vertical gradients in the velocity field. The effect can also be demonstrated with vertical velocity: If the cylinder is slowly made to rise, then the fluid immediately above it will also be pushed upward rather than flow past the cylinder—except at the water's surface, where the geostrophic flow breaks down. The fluid above the cylinder, which behaves as though it were rigidly attached to the cylinder, is called a *Taylor column.*
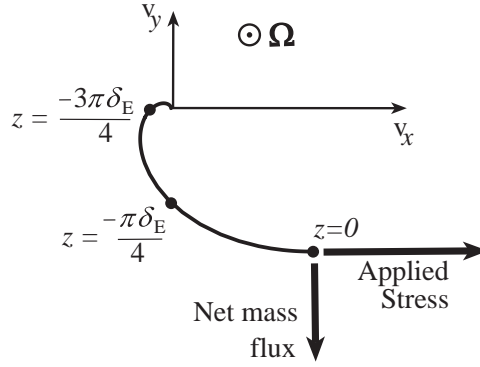
14.5.4 Ekman Boundary Layers

As we have seen, Ekman numbers are typically very small in the bulk of a rotating fluid. However, as was true in the absence of rotation, the no slip condition at a solid surface generates a boundary layer that can indirectly impose a major influence on the global velocity field.

When the Rossby number is smaller than one, the structure of a laminar boundary layer is dictated by a balance between viscous and Coriolis forces rather than viscous and inertial forces. Balancing the relevant terms in Eq. (14.51a), we obtain an estimate of the boundary-layer thickness:

$$\boxed{\text{thickness} \sim \delta_E \equiv \sqrt{\frac{\nu}{\Omega}}} . \tag{14.58}$$

In other words, the thickness of the boundary layer is that which makes the layer's Ekman number unity, $\mathrm{Ek}(\delta_E) = \nu/(\Omega\delta_E^2) = 1$.

Fig. 14.14: Ekman spiral at the ocean surface, where the wind exerts a stress.

Consider such an "Ekman boundary layer" at the bottom or top of a layer of geostrophically flowing fluid. For the same reasons as we met in the case of ordinary laminar boundary layers, the generalized pressure P' will be nearly independent of height z through the Ekman layer; i.e. it will have the value dictated by the flow just outside the layer: $\nabla P' = -2\rho\mathbf{\Omega} \times \mathbf{V} = \text{constant}$. Here $\mathbf{V}$ is the velocity just outside the layer (the velocity of the bulk flow), which we assume to be constant on scales $\sim \delta_E$. Since $\mathbf{\Omega}$ is vertical, $\nabla P'$ like $\mathbf{V}$ will be horizontal, i.e., they will lie in the x, y plane. To simplify the analysis, we introduce the fluid velocity relative to the bulk flow,

$$\mathbf{w} \equiv \mathbf{v} - \mathbf{V} \ , \tag{14.59}$$

which goes to zero outside the boundary layer. When rewritten in terms of $\mathbf{w}$, the Navier Stokes equation (14.51a) [with $\nabla P'/\rho = -2\mathbf{\Omega} \times \mathbf{V}$ and with $d\mathbf{v}/dt = \partial\mathbf{v}/\partial t + (\mathbf{v} \cdot \nabla)\mathbf{v} = 0$ because the flow in the thin boundary layer is steady and $\mathbf{v}$ is horizontal and varies only vertically] takes the simple form $d^2\mathbf{w}/dz^2 = (2/\nu)\mathbf{\Omega} \times \mathbf{w}$. Choosing Cartesian coordinates with an upward vertical z direction, assuming $\mathbf{\Omega} = +\Omega\mathbf{e}_z$ (as is the case for the oceans and atmosphere in the northern hemisphere), and introducing the complex quantity

$$w = w_x + iw_y \ , \tag{14.60}$$

to describe the horizontal velocity field, we can rewrite $d^2\mathbf{w}/dz^2 = (2/\nu)\mathbf{\Omega} \times \mathbf{w}$ as

$$\frac{d^2w}{dz^2} = \frac{2i}{\delta_E^2}w = \left(\frac{1+i}{\delta_E}\right)^2 w \ . \tag{14.61}$$

This must be solved subject to $w \to 0$ far from the water's boundary and some appropriate condition at the boundary.

For a first illustration of an Ekman layer, consider the effects of *a wind blowing in the* $\mathbf{e}_x$ *direction above a still ocean* and set $z = 0$ at the ocean's surface. The wind will exert, through a turbulent boundary layer of air, a stress T_{xz} on the ocean's surface, and this must be balanced by an equal, viscous stress $\nu\rho dw_x dz$ at the top of the water's boundary layer, $z = 0$. Thus, there must be a velocity gradient, $dw_x/dz = T_{xz}/\nu\rho$ in the water at $z = 0$. (This replaces the "no slip" boundary condition that we have when the boundary is a solid
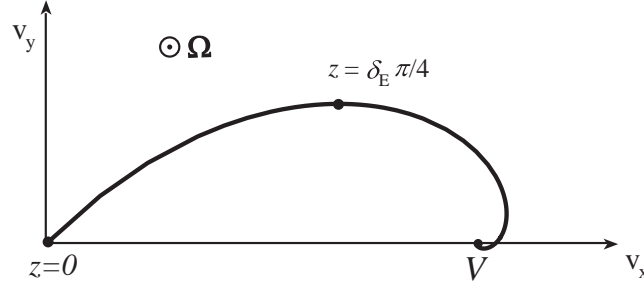
Fig. 14.15: Ekman Spiral in the bottom boundary layer, when the bulk flow above it moves geostrophically with speed $V\mathbf{e}_x$. .

surface.) Imposing this boundary condition along with $w \to 0$ as $z \to -\infty$ (down into the ocean), we find from Eqs. (14.61) and (14.60):

$$v_x - V = w_x = \left(\frac{T_{xz}\delta_E}{\sqrt{2}\,\nu\rho} \right) e^{z/\delta_E} \cos(z/\delta_E - \pi/4) \, ,$$

$$v_y = w_y = \left(\frac{T_{xz}\delta_E}{\sqrt{2}\,\nu\rho} \right) e^{z/\delta_E} \sin(z/\delta_E - \pi/4) \, , \tag{14.62}$$

for $z \le 0$; cf. Fig. 14.14. As a function of depth, this velocity field has the form of a spiral—the so-called *Ekman spiral*. When $\boldsymbol{\Omega}$ points toward us (as in Fig. 14.14), the spiral is clockwise and tightens as we move away from the boundary ($z = 0$ in the figure) into the bulk flow.

By integrating the mass flux $\rho\mathbf{v}$ over z, we find for the total mass flowing per unit time per unit length of the ocean's surface

$$\mathbf{F} = \rho \int_{-\infty}^{0} \mathbf{v}\,dz = -\frac{\delta_E^2}{2\nu}T_{xz}\mathbf{e}_y; \tag{14.63}$$

see Fig. 14.14. Thus, the wind, blowing in the $\mathbf{e}_x$ direction, causes a net mass flow in the direction of $\mathbf{e}_x \times \boldsymbol{\Omega}/\Omega = -\mathbf{e}_y$. This response (called "Ekman pumping") may seem less paradoxical if one recalls how a gyroscope responds to applied forces.

This mechanism is responsible for the creation of *gyres* in the oceans; cf. Ex. 14.12 and Fig. 14.16 below.

As a second illustration of an Ekman boundary layer, we consider a geostrophic flow with nonzero velocity $\mathbf{V} = V\mathbf{e}_x$ in the bulk of the fluid, and we examine this flow's interaction with a static, solid surface at its bottom. We set $z = 0$ at the bottom, with z increasing upward, in the $\boldsymbol{\Omega}$ direction. The structure of the boundary layer on the bottom is governed by the same differential equation (14.61) as at the wind-blown surface, but with altered boundary conditions. The solution is

$$v_x - V = w_x = -V \exp(-z/\delta_E) \cos(z/\delta_E) \, , \quad v_y = w_y = +V \exp(-z/\delta_E) \sin(z/\delta_E) \, . \tag{14.64}$$

This solution is shown in Fig. 14.15.
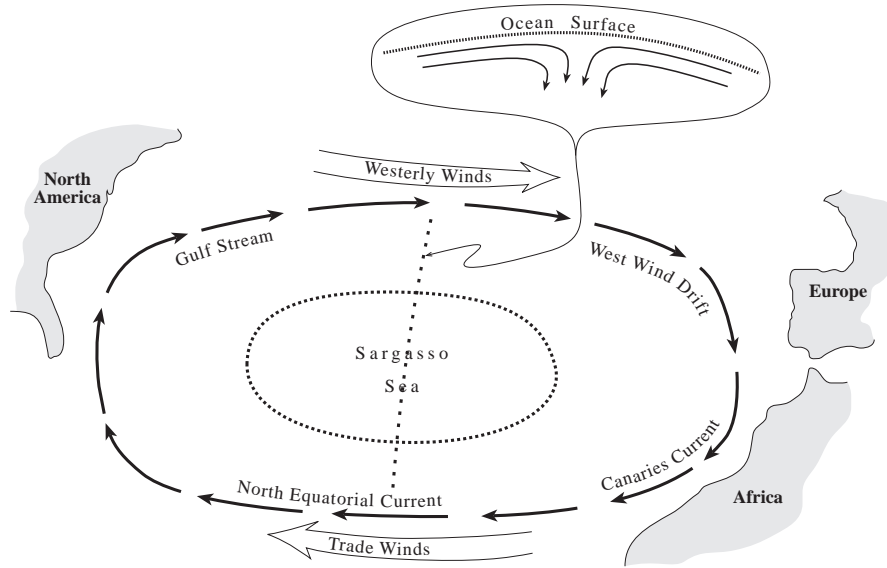
Fig. 14.16: Winds and ocean currents in the north Atlantic. The upper inset shows the surface currents, along the dotted north-south line, that produce the Sargasso-Sea gyre.

Recall that we have assumed $\boldsymbol{\Omega}$ points in the upward $+z$ direction, which is appropriate for the ocean and atmosphere in the northern hemisphere. If, instead, $\boldsymbol{\Omega}$ points downward (as in the southern hemisphere), then the handedness of the Ekman spiral is reversed.

Ekman boundary layers are important because they can circulate rotating fluids faster than viscous diffusion. Suppose we have a nonrotating container (e.g., a tea cup) of radius L, containing a fluid that rotates with angular velocity Ω (e.g., due to stirring; cf. Ex. 14.13). As you will see in your analysis of Ex. 14.13, the Ekman layer at the container's bottom experiences a pressure difference between the wall and the container's center given by $\Delta P \sim \rho L^2 \Omega^2$. This drives a fluid circulation in the Ekman layer, from the wall toward the center, with radial speed $V \sim \Omega L$. The circulating fluid must upwell at the bottom's center from the Ekman layer into the bulk fluid. This produces a poloidal mixing of the fluid on a timescale given by

$$t_E \sim \frac{L^3}{L\delta_E V} \sim \frac{L\delta_E}{\nu} \, . \tag{14.65}$$

This is shorter than the timescale for simple diffusion of vorticity, $t_\nu \sim L^2/\nu$, by a factor $t_E/t_\nu \sim \sqrt{\text{Ek}}$, which as we have seen can be very small. This circulation and mixing are key to the piling up of tea leaves at the bottom center of a stirred tea cup, and to the mixing of the tea or milk into the cup's hot water; cf. Ex. 14.13.

This circulation, driven by an Ekman layer, is an example of a *secondary flow* — a weakly perturbative bulk flow that is produced by interaction with a boundary. For other examples of secondary flows, see Taylor (1964b).

****

EXERCISES

Exercise 14.12 ****Example: Winds and Ocean Currents in the North Atlantic*
In the north Atlantic Ocean there is the pattern of winds and ocean currents shown in
Fig. 14.16. Westerly winds blow from west to east at 40 degrees latitude. Trade winds blow
from east to west at 20 degrees latitude. In between, around 30 degrees latitude, is the
Sargasso Sea: A 1.5-meter high gyre (raised hump of water). The gyre is created by ocean
surface currents, extending down to a depth of only about 30 meters, that flow northward
from the trade-wind region and southward from the westerly wind region; see the upper
inset in Fig. 14.16. A deep ocean current, extending from the surface down to near the
bottom, circulates around the Sargasso-Sea gyre in a clockwise manner. This current goes
under different names in different regions of the ocean: gulf stream, west wind drift, Canaries
current, and north equatorial current. Explain both qualitatively and semiquantitatively (in
order of magnitude) how the winds are ultimately responsible for all these features of the
ocean. More specifically,

(a) Explain the surface currents in terms of an Ekman layer at the top of the Ocean, with
thickness δ_E about 30 meters. From this measured δ_E compute the kinematic viscosity
ν in the boundary layer. Your result should be far larger than the ν for water (Table
13.2). The reason is that the boundary layer is turbulent, and its eddies produce this
large viscosity; see Sec. 15.4.2 of the next chapter.

(b) Explain why the height of the gyre that the surface currents produce in the Sargasso
Sea is about 1.5 meters.

(c) Explain the deep ocean current (gulf stream etc.) in terms of a geostrophic flow, and
estimate the speed of this current. Note: this current, like circulation in a tea cup, is
an example of a "secondary flow".

(d) If there were no continents on Earth, but only an ocean of uniform depth, what would
be the flow pattern of this deep current—it's directions of motion at various locations
around the Earth, and its speeds? The continents (North America, Europe, Africa)
must be responsible for the deviation of the actual current (gulf stream, etc.) from this
continent-free flow pattern. How do you think the continents give rise to the altered
flow pattern ?

Exercise 14.13 ****Example: Circulation in a Tea Cup*
Place tea leaves and water in a tea cup or glass or other, larger container. Stir the water
until it is rotating uniformly, and then stand back and watch the motion of the water and
leaves. Notice that the tea leaves tend to pile up at the cup's center. An Ekman boundary
layer on the bottom of the cup is responsible for this. In this exercise you will explore the
origin and consequences of this Ekman layer.

(a) Evaluate the pressure distribution $P(\varpi, z)$ in the bulk flow (outside all boundary lay-
ers), assuming that it rotates rigidly. (Here z is height and ϖ is distance from the
water's rotation axis.) Perform your evaluation in the water's rotating reference frame.
From this $P(\varpi, z)$ deduce the shape of the top surface of the water. Compare your
deduced shape with the actual shape in your experiment.

(b) Estimate the thickness of the Ekman layer at the bottom of your container. It is very thin. Show, using the Ekman spiral diagram, that the water in this Ekman layer flows inward toward the container's center, causing the tea leaves to pile up at the center. Estimate the radial speed of this Ekman-layer flow and the mass flux that it carries.

(c) To get a simple physical understanding of this inward flow, examine the radial gradient $\partial P/\partial \varpi$ of the pressure P in the bulk flow just above the Ekman layer. Explain why $\partial P/\partial \varpi$ in the Ekman layer will be the same as in the rigidly rotating flow above it. Then apply force balance in an inertial frame to deduce that the water in the Ekman layer will be accelerated inward toward the center.

(d) Using geostrophic-flow arguments, deduce the fate of the boundary-layer water after it reaches the center of the container's bottom: where does it go? What is the large-scale circulation pattern that results from the "driving force" of the Ekman layer's mass flux? What is the Rossby number for this large-scale circulation pattern? How and where does water from the bulk, nearly rigidly rotating flow, enter the bottom boundary layer so as to be swept inward toward the center?

(d) Explain how this large-scale circulation pattern can mix much of the water through the boundary layer in the time t_E of Eq. (14.65). What is the value of this t_E for the water in your container? Explain why this, then, must also be the time for the angular velocity of the bulk flow to slow substantially. Compare your computed value of t_E with the observed slow-down time for the water in your container.

Exercise 14.14 ***Example: Water Going Down a Shower Drain*

(a) In a shower or bathtub with the drain somewhere near the center, not the wall, set water rotating so a whirlpool forms over the drain.[4] Perform an experiment to see where the water going down the drain comes from: the surface of the water, its bulk, or its bottom. For example, you could sprinkle baby powder on the top of the water, near the whirlpool, and measure how fast the powder is pulled inward and down the drain; put something neutrally buoyant in the bulk and watch its motion; and put sand on the bottom of the shower near the whirlpool and measure how fast the sand is pulled inward and down the drain.

(b) Explain the result of your experiment. How is it related to the tea cup problem, Ex. 14.13?

(c) Compute the shape of the surface of the water near and in the whirlpool.

****

---

[4]Incidentally, in a bathtub or shower, the magnitude of the Coriolis force resulting from the earth's rotation with angular velocity Ω_* is a fraction $\sim \Omega_*(\varpi/g)^{1/2} \sim 3 \times 10^{-6}$ of the typical centrifugal force in the whirlpool (where g is the acceleration of gravity and $\varpi \sim 2$ cm is the radius of the vortex at the point where the water's surface achieves an appreciable downward slope). Thus, only under the most controlled of conditions will the hemisphere in which the drainhole is located influence the direction of rotation. It is trivially easy for you to make the whirlpool turn in whichever direction you wish.

14.6 $\boxed{\text{T2}}$ Instabilities of Shear Flows — Billow Clouds,f Turbulence in the Stratosphere

In this section we shall explore the stability of a variety of shear flows. We shall begin with the simplest case of two incompressible fluids, one above the other, that move with different uniform speeds, with gravity negligible. Such a flow has a delta function spike of vorticity at the interface between the fluids, and, as we shall see, the interface is always unstable. This is the *Kelvin-Helmholtz instability*. We shall then explore the ability of gravity to suppress this instability. If the densities of the two fluids are nearly the same, there is no suppression, which is why the Kelvin-Helmholtz instability is seen in a variety of places in the Earth's atmosphere and oceans. Finally, we shall allow the density and horizontal velocity to change continuously, vertically, e.g., in the earth's stratosphere, and for such a flow we shall deduce the *Richardson criterion for instability*, which is often satisfied in the stratosphere, leading to turbulence. Along the way we shall briefly visit several other instabilities that occur in stratified fluids.

14.6.1 $\boxed{\text{T2}}$ Discontinuous Flow: Kelvin-Helmholtz Instability

A particularly interesting, simple type of vorticity distribution is one where the vorticity is confined to a thin, plane interface between two immiscible fluids. In other words, one fluid is in uniform motion relative to the other. This type of flow arises quite frequently; for example, when the wind blows over the ocean or when smoke from a smokestack discharges into the atmosphere (a flow that is locally planar but not globally). Following the discussion of the previous section, we expect that a boundary layer will form at the interface and the vorticity will slowly diffuse away from it. However, quite often the boundary layer is much thinner than the length scale associated with the flow and we can therefore treat it as a plane discontinuity in the velocity field. We shall analyze the stability of this flow, initially without gravity (this subsection), then with gravity present (next subsection). Our analysis will provide another illustration of the behavior of vorticity as well as an introduction to techniques that are commonly used to analyze fluid instabilities.

We shall restrict attention to the simplest version of this flow: an equilibrium with a fluid of density ρ_+ moving horizontally with speed V above a second fluid, which is at rest, with density ρ_-. We let x be a coordinate measured along the planar interface in the direction of the flow, and let y be measured perpendicular to it. The equilibrium contains a sheet of vorticity lying in the plane $y = 0$, across which the velocity changes discontinuously. Now, this discontinuity ought to be treated as a boundary layer, with a thickness determined by the viscosity. However, in this problem, we shall analyze disturbances with length scales much greater than the thickness of the boundary layer. A corollary of this assumption is that we can ignore viscous stresses in the body of the flow. We also specialise to very subsonic speeds, for which the flow can be treated as incompressible, and we ignore the effects of surface tension as well as gravity.

A full description of this flow requires solving the full equations of fluid dynamics, which are quite non-linear and, it turns out, for this problem can only be solved numerically. However, we can make progress analytically on an important sub-problem. This is the issue

of whether or not this equilibrium flow is stable to small perturbations. To answer this question, we linearize the fluid equations in the amplitude of the perturbations.

We consider a small vertical perturbation $\xi(x,t)$ in the location of the interface [Fig. 14.17(a) below]. We denote the associated perturbations to the pressure and velocity by $\delta P, \delta \mathbf{v}$. That is, we write

$$P(\mathbf{x},t) = P_0 + \delta P(\mathbf{x},t) , \quad \mathbf{v} = VH(y)\mathbf{e}_x + \delta \mathbf{v}(\mathbf{x},t) , \tag{14.66}$$

where P_0 is the constant pressure in the equilibrium flow about which we are perturbing, V is the constant speed of the flow above the interface, and $H(y)$ is the Heaviside step function (1 for $y > 0$ and 0 for $y < 0$). We substitute these $P(\mathbf{x},t)$ and $\mathbf{v}(\mathbf{x},t)$ into the governing equations: the incompressibility relation

$$\boldsymbol{\nabla} \cdot \mathbf{v} = 0 , \tag{14.67}$$

and the viscosity-free Navier Stokes equation, i.e., the Euler equation,

$$\frac{d\mathbf{v}}{dt} = \frac{-\boldsymbol{\nabla} P}{\rho} . \tag{14.68}$$

We then subtract off the equations satisfied by the equilibrium quantities to obtain, for the perturbed variables,

$$\boldsymbol{\nabla} \cdot \delta \mathbf{v} = 0, \tag{14.69}$$

$$\frac{d\delta \mathbf{v}}{dt} = -\frac{\boldsymbol{\nabla} \delta P}{\rho} . \tag{14.70}$$

Combining these two equations we find, as for Stokes flow (Sec. 14.3.2), that the pressure satifies Laplace's equation

$$\nabla^2 \delta P = 0 . \tag{14.71}$$

We now follow the procedure that we used in Sec. 12.4.2 when treating Rayleigh waves on the surface of an elastic medium: we seek a wave mode in which the perturbed quantities vary $\propto \exp[i(kx - \omega t)]f(y)$ with $f(y)$ dying out away from the interface. From Laplace's equation (14.71), we infer an exponential falloff with $|y|$:

$$\delta P = \delta P_0 e^{-k|y|+i(kx-\omega t)} , \tag{14.72}$$

where δP_0 is a constant.

Our next step is to substitute this δP into the perturbed Euler equation (14.70) to obtain

$$\delta v_y = \frac{ik\delta P}{(\omega - kV)\rho_+} \quad \text{at } y > 0 , \qquad \delta v_y = \frac{-ik\delta P}{\omega \rho_-} \quad \text{at } y < 0 . \tag{14.73}$$

We must impose two boundary conditions at the interface between the fluids: continuity of the vertical displacement ξ of the interface (the tangential displacement need not be continuous since we are examining scales large compared to the boundary layer), and continuity of the pressure P across the interface. [See Eq. (12.49) and associated discussion for the analogous boundary conditions at a discontinuity in an elastic medium.] Now, the vertical

interface displacement ξ is related to the velocity perturbation by $d\xi/dt = \delta v_y(y = 0)$, which implies by Eq. (14.73) that

$$\xi = \frac{i\delta v_y}{(\omega - kV)} \quad \text{at } y = 0_+ \quad \text{(immediately above the interface,)}$$

$$\xi = \frac{i\delta v_y}{\omega} \quad \text{at } y = 0_- \quad \text{(immediately below the interface).} \tag{14.74}$$

Then, by virtue of Eqs. (14.72), (14.74), and (14.73), the continuity of pressure and vertical displacement at $y = 0$ imply that

$$\rho_+(\omega - kV)^2 + \rho_-\omega^2 = 0 , \tag{14.75}$$

where ρ_+ and ρ_- are the densities of the fluid above and below the interface. Solving for frequency ω as a function of horizontal wave number k, we obtain the following *dispersion relation for linear Kelvin-Helmholtz modes:*

$$\boxed{\omega = kV \left(\frac{\rho_+ \pm i(\rho_+\rho_-)^{1/2}}{\rho_+ + \rho_-} \right).} \tag{14.76}$$

This dispersion relation can be used to describe both a sinusoidal perturbation whose amplitude grows in time, and a time independent perturbation that grows spatially:

Temporal growth

Suppose that we create some small, localized disturbance at time $t = 0$. We can Fourier analyze the disturbance in space and, as we have linearized the problem, can consider the temporal evolution of each Fourier component separately. Now, what we ought to do is to solve the initial value problem carefully taking account of the initial conditions. However, when there are growing modes, we can usually infer the long-term behavior by ignoring the transients and just consider the growing solutions. In our case, we infer from Eqs. (14.72), (14.73), (14.74) and the dispersion relation (14.76) that a mode with spatial frequency k must grow as

$$\delta P, \, \xi \propto \exp \left[\left(\frac{kV(\rho_+\rho_-)^{1/2}}{(\rho_+ + \rho_-)} \right) t + ik \left(x - V\frac{\rho_+}{\rho_+ + \rho_-}t \right) \right] \tag{14.77}$$

Thus, *this mode grows exponentially with time* (Fig. 14.17a). Note that the mode is non-dispersive, and if the two densities are equal, it e-folds in a few periods. This means that the fastest modes to grow are those which have the shortest periods and hence the shortest wavelengths. (However, the wavelength must not approach the thickness of the boundary layer and thereby compromise our assumption that the effects of viscosity are negligible.)

We can understand this growing mode somewhat better by transforming into the center of momentum frame, which moves with speed $\rho_+V/(\rho_+ + \rho_-)$ relative to the frame in which the lower fluid is at rest. In this (primed) frame, the velocity of the upper fluid is $V' = \rho_-V/(\rho_+ + \rho_-)$ and so the perturbations evolve as

$$\delta P, \, \xi \propto \exp[kV'(\rho_+/\rho_-)^{1/2}t] \cos(kx') \tag{14.78}$$

In this frame the wave is purely growing, whereas in our original frame it oscillated with time as it grew.
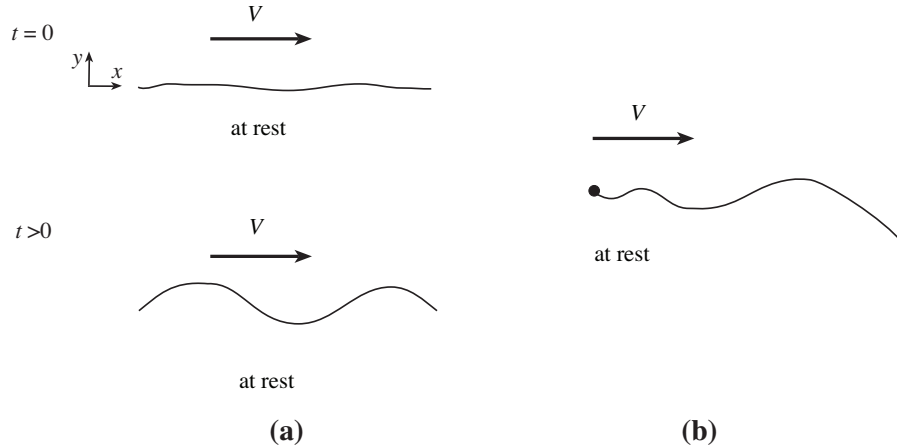
Fig. 14.17: Kelvin-Helmholtz Instability. a) Temporarily growing mode. b) Spatially growing mode.

Spatial Growth

An alternative type of mode is one in which a small perturbation is excited temporally at some point where the shear layer begins [Fig. 14.17b]. In this case we regard the frequency ω as real and look for the mode with positive imaginary k corresponding to spatial growth. Using Eq. (14.76), we obtain

$$k = \frac{\omega}{V} \left[1 \pm i \left(\frac{\rho_-}{\rho_+} \right)^{1/2} \right] . \tag{14.79}$$

The mode therefore grows exponentially with distance from the point of excitation.

ROGER: I HAVE COMMENTED OUT A SECTION HERE; PLEASE LOOK AT IT TO UNDERSTAND WHY, AND THEN FIX IT IF YOU DISAGREE. – KIP

Physical Interpretation of the Instability

We have performed a normal mode analysis of a particular flow and discovered that there are unstable modes. However much we calculate the form of the growing modes, though, we cannot be said to understand the instability until we can explain it physically. In the case of the Kelvin-Helmholtz instability, this is a simple task.

The flow pattern is shown schematically in Fig. 14.18. The upper fluid will have to move faster when passing over a crest in the water wave as the cross sectional area of a flow tube diminishes and the flux of fluid must be conserved. By Bernoulli's theorem, the upper pressure will be lower than ambient at this point and so the crest will rise even higher. Conversely in the trough of the wave, the upper fluid will travel slower and its pressure will increase. The pressure differential will push the trough downward, making it grow.

Equivalently, we can regard the boundary layer as a plane containing parallel vortex lines which interact one with another, much like magnetic field lines exert pressure on one another.

When the vortex lines all lie strictly in a plane, they are in equilibrium as the repulsive force exerted by one on its neighbor is balanced by an opposite force exerted by the opposite neighbor. However, when this equilibrium is disturbed, the forces become unbalanced and the vortex sheet effectively buckles.

More generally, whenever there is a large amount of relative kinetic energy available in a large Reynolds number flow, there exists the possibility of unstable modes that can tap this energy and convert it into a spectrum of growing modes, which can then interact non-linearly to create fluid turbulence, which ultimately is dissipated as heat. However, the fact that free kinetic energy is available does not necessarily imply that the flow is unstable; sometimes it is stable. Instability must be demonstrated, often a very difficult task.

14.6.2 $\boxed{\text{T2}}$ Discontinuous Flow with Gravity

What happens to this Kelvin-Helmholtz instability if we turn on gravity? To learn the answer, we insert a downward gravitational acceleration $\boldsymbol{g}$ into the above analysis. The result (Ex. 14.15) is the following modification of the dispersion relation (14.76):

$$\frac{\omega}{k} = \frac{\rho_+ V}{\rho_+ + \rho_-} \pm \left[\frac{g}{k} \left(\frac{\rho_- - \rho_+}{\rho_+ + \rho_-} \right) - \frac{\rho_+ \rho_-}{(\rho_+ + \rho_-)^2} V^2 \right]^{1/2} . \tag{14.80}$$

If the lower fluid is sufficiently more dense than the upper fluid (ρ_- sufficiently bigger than ρ_+), then gravity g will change the sign of the quantity inside the square root, making ω/k real, which means the Kelvin-Helmholtz instability is suppressed. In other words, *in order for the flow to be Kelvin-Helmholtz unstable in the presence of gravity, the two fluids must have nearly the same density:*

$$\left| \frac{\rho_- - \rho_+}{\rho_+ + \rho_-} \right| \ll \frac{\rho_+ \rho_-}{(\rho_+ + \rho_-)^2} \frac{kV^2}{g} . \tag{14.81}$$

This is the case for many interfaces in Nature, which is why the Kelvin-Helmholtz instability is often seen. An example is the interface between a water-vapor-ladened layer of air overlain by a fast-moving, dryer layer, and the result is the so-called "billow clouds" shown in Fig. 14.19. Other examples are flow interfaces in the ocean, and the edges of dark smoke pouring out of a smoke stack.
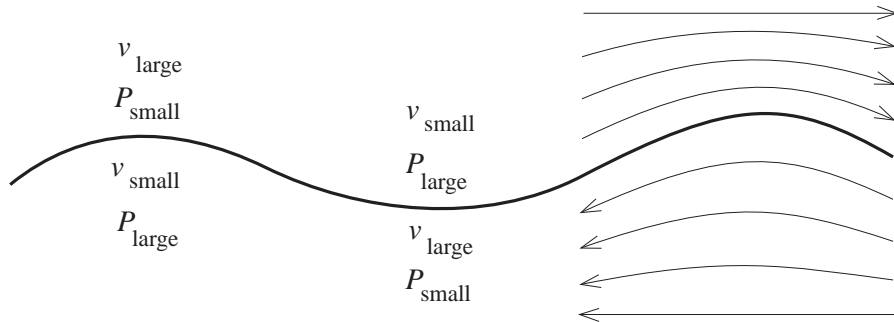
Fig. 14.18: Physical explanation for the Kelvin-Helmholtz instability.

Fig. 14.19: Billow clouds above San Francisco, photographed by Mila Zinkova. The cloud structure is generated by the Kelvin-Helmholtz instability. It is thought that these types of billow clouds may have inspired the swirls in Vincent van Gogh's famous painting "Starry Night".

As another application of the dispersion relation (14.80), consider the excitation of ocean waves by a laminar-flowing wind. In this case, the "+" fluid is air and the "−" fluid is water, so the densities are very different: $\rho_+/\rho_- \simeq 0.001$. The instability criterion (14.81) tells us the minimum wind velocity V required to make the waves grow:

$$V_{\min} \simeq \left(\frac{g}{k}\frac{\rho_+ -_-}{\rho_+}\right)^{1/2} \simeq 450 \mathrm{km\,h}^{-1}\sqrt{\lambda/10\mathrm{m}}\,, \tag{14.82}$$

where $\lambda = 2\pi/k$ is the waves' wavelength.

Obviously, this answer is wrong, physically. Water waves are easily driven by winds that are far slower than this. Evidently, some other mechanism of interaction between wind and water must drive the waves much more strongly. Observations of wind over water reveal the answer: The winds near the sea's surface are typically quite turbulent, not laminar. The randomly fluctuating pressures in a turbulent wind are far more effective than the smoothly varying pressure of a laminar wind, in driving ocean waves. For details, see Phillips (1957).

As another, very simple application of the dispersion relation (14.80), set the speed V of the upper fluid to zero. In this case, the interface is unstable if and only if the upper fluid has higher density than the lower fluid, $\rho_+ > \rho_-$. This is called the *Rayleigh-Taylor instability* for incompressible fluids.

****

EXERCISES

**Exercise 14.15** $\boxed{T2}$ *Problem: Discontinuous Flow with Gravity*
Insert gravity into the analysis of the Kelvin-Helmholtz instability (with the uniform gravitational acceleration $\boldsymbol{g}$ pointing orthogonal to the fluid interface, from the upper "+" fluid to the lower "−" fluid. Thereby derive the dispersion relation(eq14n:GravNotImportant).

****

14.6.3 $\boxed{\text{T2}}$ Smoothly Stratified Flows: Rayleigh and Richardson Criteria for Instability.

Sometimes one can diagnose a fluid instability using simple physical arguments rather than detailed mathematical analysis. We conclude this chapter with two examples.

First, we consider rotating *Couette flow*, i.e. the azimuthal flow of an incompressible, effectively inviscid fluid, rotating axially between two coaxial cylinders (Fig 14.20).
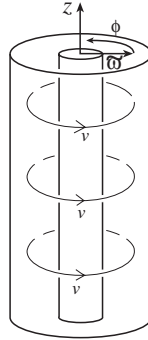
Fig. 14.20: Rotating Couette flow.

We shall explore the stability of this flow to purely axisymmetric perturbations by using a thought experiment in which we interchange two fluid rings. As there are no azimuthal forces (no forces in the ϕ direction), the interchange will occur at constant angular momentum per unit mass. Now, suppose that the ring that moves outward in radius ϖ has lower specific angular momentum j than the surroundings into which it has moved; then it will have less centrifugal force per unit mass j^2/ϖ^3 than its surroundings and will thus experience a restoring force that drives it back to its original position. Conversely, if the surroundings' angular momentum per unit mass decreases outward, then the displaced ring will continue to expand. We conclude on this basis that *Couette and similar flows are unstable when the angular momentum decreases outward.* This is known as the *Rayleigh criterion.* We shall return to Couette flow in Chap. 15.

Compact stellar objects (black holes, neutron stars and white dwarfs) are sometimes surrounded by orbiting *accretion disks* of gas. The gas in these disks orbits roughly with the angular velocity dictated by Kepler's laws. Therefore the specific angular momentum of the gas increases radially outward, proportional to the square root of the orbital radius. Consequently accretion disks are stable to this type of instability.

For our second example of a simple physical diagnosis of instability, consider the situation analyzed in Ex. 14.15 (Kelvin-Helmholtz instability with gravity present), but with the density and velocity changing continuously instead of discontinuously, as one moves upward. More specifically, focus on the earth's stratosphere, which extends from ~ 10 km height to ~ 40 km. The density in the stratosphere decreases upward faster than if the stratosphere were isentropic. This means that, when a fluid element moves upward adiabatically, its pressure-induced density reduction is smaller than the density decrease in its surroundings. Since it is now more dense than its surroundings, the downward pull of gravity on the fluid

element will exceed the upward buoyant force, so the fluid element will be pulled back down. This means that the stratosphere is stably stratified.

It may be possible, however, for the stratosphere to tap the relative kinetic energy in its horizontal winds, so as to mix the air vertically. Consider the pedagogical example of two thin stream tubes of horizontally flowing air in the stratosphere, separated vertically by a distance $\delta\ell$ large compared to their thicknesses. The speed of the upper stream will exceed that of the lower stream by $\delta V = V'\delta\ell$, where $V' = dV/dz$ is the velocity gradient. In the center of velocity frame, the streams each have speed $\delta V/2$ and they differ in density by $\delta\rho = |\rho'\delta\ell|$. To interchange these streams requires doing a work per unit mass[5] $\delta W = g(\delta\rho/2\rho)\delta\ell$ against gravity (where the factor 2 comes from the fact that there are two unit masses involved in the interchange, one going up and the other coming down). This work can be supplied by the streams' kinetic energy, if the available kinetic energy per unit mass $\delta E_k = (\delta V/2)^2/2$ exceeds the required work. *A necessary condition for instability* is then that

$$\delta E_k = (\delta V)^2/8 > \delta W = g|\rho'/2\rho|\delta\ell^2 \tag{14.83}$$

or

$$\boxed{\mathrm{Ri} = \frac{|\rho'|g}{\rho V'^2} < \frac{1}{4}} \tag{14.84}$$

where $V' = dV/dz$ is the velocity gradient. This is known as the *Richardson criterion for instability*, and Ri is the *Richardson number*. Under a wide variety of circumstances this criterion turns out to be sufficient for instability.

The density scale height in the stratosphere is $\rho/|\rho'| \sim 10$ km. Therefore the maximum velocity gradient allowed by the Richardson criterion is

$$V' \lesssim 60\frac{\mathrm{m\ s^{-1}}}{\mathrm{km}} \ . \tag{14.85}$$

Larger velocity gradients are rapidly disrupted by instabilities. This instability is responsible for much of the clear air turbulence encountered by airplanes and it is to a discussion of turbulence that we shall turn in the next chapter.

Bibliographic Note

Vorticity is so fundamental to fluid mechanics that it is treated in detail in all fluid dynamical textbooks. Among those we find useful are Acheson (1990) at an elementary level; and at a more advanced level Batchelor (1970), Lighthill (1986) and Landau and Lifshitz (1959); and for an especially physical approach Tritton (1977). For a textbook treatment of rotating flows and weak perturbations of them, we recommend Greenspan (1973), and for geophysical applications, Gill (1982). To build up physical intuition, we suggest the following movies: *Vorticity* by Shapiro (1961), *Low Reynolds Number Flows* by Taylor (1964a), *Fundamentals of Boundary Layers* by Abernathy (1068), *Rotating Flows* by Fultz (1969), and *Secondary Flows* by Taylor (1964b).

---

[5]Here, for simplicity we idealize the streams' densities as not changing when they move vertically — an idealization that makes gravity be more effective at resisting the instability. In the stratosphere, where the density drops vertically much faster than if it were isentropic, this idealization is pretty good.

Box 14.4
Important Concepts in Chapter 13

- Differential equation for evolution of vorticity, Sec. 14.2.1
- Circulation, Sec. 14.2.4
- Kelvin's theorem for evolution of circulation, Sec. 14.2.4
- Vortex lines, Sec. 14.2.1
- Freezing of vortex lines into the flow for barotropic, inviscid fluid, Sec. 14.2.1
- Stretching of vortex lines, e.g. in a tornado, Sec. 14.2.3
- Diffusion of vorticity due to viscosity, Sec. 14.2.5
- Processes that create vortex lines, Sec. 14.2.6
- Lift on aerofoil related to circulation around it, Ex. 14.4
- Small change of pressure across boundary layer, Sec. 14.4
- Laminar boundary layers, Sec. 14.4
- Separation of a boundary layer, Sec. 14.4.3
- Stokes flow around an obstacle at low Reynolds number, Sec. 14.3.2
- Coriolis and Centrifugal forces in rotating reference frame, Sec. 14.5.1
- Rossby number as ratio of inertial to Coriolis acceleration, Sec. 14.5.1
- Eckmann number as ratio of viscous to Coriolis acceleration, Sec. 14.5.1
- Geostrophic flows, Secs. 14.5.2, 14.5.3
- Taylor-Proudman theorem: 2-D flow orthogonal to vortex lines, Sec. 14.5.3
- Taylor column, Fig. 14.13
- Kelvin-Helmholtz instability, Sec. 14.6.1
- Richardson criterion for gravity to suppress Kelvin-Helmholtz instability, Sec. 14.6.3
- Drag force and drag coefficient, Sec. 14.4
- Rayleigh criterion for instability of rotating Couette flow, Sec. 14.6.3
- Methods of analysis

  - Order of magnitude analysis, Sec. 14.4
  - Velocity as gradient of a potential when vorticity vanishes, Secs. 14.1, 14.4
  - Stream function – vector potential for velocity in incompressible flow; becomes a scalar potential in 2-dimensional flow, Sec. 14.4
  - Computing flow details by first solving vorticity evolution equation, Ex. 14.3
  - Matched asymptotic expansions, Sec. 14.3.2
  - Similarity solution, Sec. 14.4
  - Scaling, Ex. 14.10

Bibliography

Abernathy, F. 1068. *Fundamentals of Boundary Layers*, a movie (National Committee for Fluid M echanics Films); available at `http://web.mit.edu/hml/ncfmf.html` .

Acheson, D. J. 1990. *Elementary Fluid Dynamics*, Oxford: Clarendon Press.

Batchelor, G. K. 1970. *An Introduction to Fluid Dynamics*, Cambridge: Cambridge University Press.

Feyman, R. P. 1972. *Statistical Mechanics*, Reading: Benjamin.

Fultz, D. 1969. *Rotating Flows*, a movie (National Committee for Fluid Mechanics Films); available at `http://web.mit.edu/hml/ncfmf.html` .

Greenspan, H. P. 1973. *The Theory of Rotating Fluids*, Cambridge: Cambridge University Press.

Landau, L. D. and Lifshitz, E. M. 1959. *Fluid Mechanics*, Oxford:Pergamon.

Phillips, O. M. 19576. "On the generation of waves by turbulent wind," Journal of Fluid Mechanics, **2**, 417–445.

Shapiro, A. 1961. *Vorticity*, a movie (National Committee for Fluid Mechanics Films); available in two parts at `http://web.mit.edu/hml/ncfmf.html`.

Taylor, G.I.] 1964a. *Low Reynolds Number Flows*, a movie (National Committee for Fluid Mechanics Films); available at `http://web.mit.edu/hml/ncfmf.html` .

Taylor, E.S. 1964b. *Secondary Flow*, a movie (National Committee for Fluid Mechanics Films); available at `http://web.mit.edu/fluids/www/Shapiro/ncfmf.html` .

Tritton, D. J. 1977. *Physical Fluid Dynamics*, Wokingham: van Nostrand-Reinhold.

Turco et al. 1986. *Science*, **222**, 283.

White, F. M. 1974. *Viscous Fluid Flow*, New York: McGraw-Hill.